Gondwana Research 146 (2025) 74–92

Contents lists available at ScienceDirect

Gondwana Research

journal homepage: www.elsevier.com/locate/gr

Phanerozoic evolution of Fennoscandia: Evidence from apatite fission track, fluid flow and geodynamic data in Finland and Estonia

Ilmo T. Kukkonen [a,b,*], Barry Kohn [b], Kalle Kirsimäe [c], Argo Jõeleht [c], Ling Chung [b], Malcolm McMillan [b], Samuel Boone [b,d], Andy Gleadow [b]

[a] University of Helsinki, Dept. of Geosciences and Geography, P.O. Box 68, FIN-00140 Helsinki, Finland
[b] School of Geography, Earth and Atmospheric Sciences, University of Melbourne, Parkville, Victoria 3010, Australia
[c] Department of Geology, University of Tartu, Ravila 14A, 50411 Tartu, Estonia
[d] School of Geosciences, University of Sydney, Camperdown, NSW 2050, Australia

ARTICLE INFO

Handling Editor: Jan Marten Huizenga

Keywords:
Fennoscandia
Apatite
Fission track
Sediment cover
Lithospheric flexure
Hydrothermal fluids

ABSTRACT

New apatite fission track (AFT) data from Estonia together with previously published data from Finland, all from crystalline basement drill core, constrain the Phanerozoic thermal history. Models show a consistent pattern of heating from Cambrian to end-Carboniferous, with peak paleotemperatures of 60 ± 10 °C when sediment cover was ~ 0.5 km thicker in the Baltic Paleobasin and ~ 1.5 km over Precambrian basement in Finland. Prior to the Phanerozoic, the Fennoscandia basement was exhumed to a peneplain by late Neoproterozoic. The evolution of Phanerozoic sedimentary cover can be linked to (1) the Scandinavian Silurian–Devonian Caledonian orogeny, (2) foreland basin and foreland uplift bulge development, (3) pre-drift extension and lithospheric uplift from Permo-Triassic to Cretaceous, and (4) Cenozoic rift-phase uplift following North Atlantic opening at ~ 54 Ma. In the Devonian, Caledonian mountains attained elevations of ~ 7–8 km, causing significant lithospheric elastic flexure resulting in a 6–7 km deep foreland basin and ~ 500 m of foreland bulge uplift affecting Fennoscandia and the Baltic Paleobasin. The flexure relaxed and the foredeep basin was partly inverted as the mountain range exhumed and eroded during late orogenic collapse (~400 Ma). The present shield area in Finland may have outcropped for a short time in the Devonian during the Caledonian forebulge phase but was covered shortly thereafter with sediments. The cover persisted until the final exhumation of Finland in the Mesozoic – Cenozoic. Some AFT data indicate hydrothermal disturbance by expulsion of hot fluids from the Caledonian thrust belt into the unconsolidated basal Cambrian sediments and crystalline basement. This craton-wide flow resulted in the precipitation of Devonian calcite-fluorite-Pb-Zn veins, Mississippi Valley type Pb-Zn deposits in the Swedish Caledonian front and dolomitic alteration of Ordovician-Silurian limestones in Estonia. Moreover, our model contributes to the interpretation of the evolution of topography in Norway and distribution of deep biosphere in Fennoscandia.

1. Introduction

In Precambrian cratonic areas lacking sedimentary cover, methods to reveal the younger geological history are limited. Quantitative constraints on thermal histories are provided by low temperature thermochronological (LTT) methods based on the decay of radioactive elements, such as the spontaneous fission of ^{238}U in apatite, titanite or zircon (fission-track method), or alpha-decay principally of ^{238}U and ^{232}Th in apatite and zircon (the (U-Th)/He method) (e.g., Fleischer et al., 1975; Donelick et al., 2005; Braun et al., 2006; Flowers et al, 2006; Flowers, 2009; Guenthner et al., 2013; Enkelmann and Garver, 2016; Hurford, 2019; Kohn and Gleadow, 2019). In the low temperature range (<250 °C) relevant typically for burial and exhumation within the depth range of the uppermost ca. 10 km of the continental crust, the most commonly applied methods are the fission-track method on apatite, zircon and titanite (Braun et al., 2006; Ketcham et al., 2007; Hurford, 2019) and the (U-Th)/He method on apatite and zircon (Ehlers and Farley, 2003; Flowers et al., 2006; Peyton and Carrapa, 2013).

On the other hand, sedimentary rocks and their stratigraphy and provenance analysis in surrounding onshore or offshore areas can be

* Corresponding author at: University of Helsinki, Dept. of Geosciences and Geography, P.O. Box 68, FIN-00140, Helsinki, Finland.
E-mail address: ilmo.kukkonen@helsinki.fi (I.T. Kukkonen).

https://doi.org/10.1016/j.gr.2025.05.011
Received 8 November 2024; Received in revised form 15 May 2025; Accepted 15 May 2025
Available online 16 June 2025
1342-937X/© 2025 The Author(s). Published by Elsevier B.V. on behalf of International Association for Gondwana Research. This is an open access article under the CC BY license (http://creativecommons.org/licenses/by/4.0/).

directly linked to the erosional and burial history of the continent (Riis, 1996; Doré, 1992; Doré et al., 2002; Pedersen et al., 2018). Geomorphological analysis of landscape forms and paleic surfaces contributes to the understanding of the burial and tectonic history (Riis, 1996; Lidmar-Bergström et al., 2000; Lidmar-Bergström et al., 2013; Japsen et al., 2015, Japsen et al., 2018), however, the interpretation of paleic surfaces without sedimentary cover is equivocal and a topic of much debate (Phillips, 2002; Nielsen et al., 2009a, b; Lidmar-Bergström and Bonow, 2009).

In the present work, we study the Phanerozoic history of the Fennoscandian Shield using apatite fission track (AFT) data focusing on the central part of the shield in Finland and the sediment-covered area of the basement in Estonia. In Estonia, no AFT studies have been carried out so far, while several workers have reported AFT results from the shield. AFT studies in the Fennoscandian Shield started with the pioneering work of Lehtovaara (1976). Later contributions include Rohrman (1995), Larson et al. (1999), Cederbom et al. (2000), Murrell (2003), Lorencak (2003), Murrell and Andriessen (2004), Kohn et al. (2009), and Green et al. (2022). Common to all these studies are the relatively old AFT ages obtained, ranging from ca. 300 Ma to more than 1,000 Ma. However, the inverted and interpreted thermal histories reported differ. Most researchers have suggested relatively simple time–temperature (t-T) histories with rather monotonous cooling trends (e.g., Larson et al., 1999; Cederbom et al., 2000; Kohn et al. 2009), but more complicated interpretations have also emerged with two warming-cooling episodes (Murrell, 2003; Murrell and Andriessen, 2004) and up to ten warming-cooling events during the last one billion years (Green et al., 2022). These differences arise mostly from the inherent ambiguity of inversion modeling of AFT data (Kohn et al., 2024), properties of the applied modelling algorithms (Vermeesch and Tian, 2014; Vermeesch, 2017; Gallagher and Ketcham, 2018), complexities of the applied fission track annealing models (Ketcham et al., 2007, Ketcham et al., 2009) and geological constraints applied in modeling (Murray et al., 2022; Abbey et al., 2023).

Finland represents the central part of the Precambrian Fennoscandian shield outcropping today (Gaál and Gorbatschev, 1987; Koistinen et al., 2001; Lehtinen et al., 2005; Kohonen and Rämö, 2005; Lahtinen et al., 2023), while Estonia at the southern margin of the shield is the northern part of the Baltic paleobasin with up to a few hundred meters of Ediacaran – Devonian sediments (Raukas & Teedumäe, 1997; Šliaupa and Hoth, 2011). An open question remains as to how and when the present shield area became exhumed and outcropped. In this work we aim to address the following questions: Was there a sedimentary cover in Finland during the Phanerozoic, if so, was it thin (<1 km) or thick (up to 3–4 km)? What were the burial and exhumation histories? How do AFT results from Estonia and Finland compare?

We use both novel and published AFT data (Green et al., 2022) from Finland and Estonia in our analysis and present a comprehensive geological model which honors the AFT data as the best constrained of the LTT methods. We show that the t-T history of the area is linked to the collisional Caledonian orogeny in the Silurian – Devonian and the development of its associated foreland basin and foredeep bulge. Further, the AFT data are consistent with the pre-drift stage lithospheric extension of western Fennoscandia in the Permian – Jurassic and the rift stage extension in the Cenozoic during and after opening of the North Atlantic. Our model explains the shield-wide Devonian hydrothermal effects expressed by the presence of calcite-fluorite-sphalerite-galena veins in the shield, dolomitization of limestones in Estonia, and Devonian paleomagnetic remanences in the shield and Estonia. Our model also contributes to the origin of present topography in Norway. Finally, we discuss the distribution and transport of microbial life forms by orogenic processes.

2. Geological overview of Fennoscandia and the Baltic paleobasin

The Fennoscandian Shield outcrops in Finland, Sweden, Norway and NW Russia (Koistinen et al., 2001; Lehtinen et al., 2005; Lahtinen et al., 2023; Fig. 1). Precambrian rocks are present under sedimentary cover in the Russian Platform (East European Platform) including the Baltic Paleobasin from Fennoscandia to the Urals in the east and the Ukrainian Shield in the south (Nikishin et al., 1996; Kheraskova et al., 2002). The Fennoscandian Shield, and the Sarmatian and Volgo-Uralian lithosphere blocks (Bogdanova et al., 2006) form a huge piece of Precambrian lithosphere (Baltica) amalgamated already in the Proterozoic (Elming et al., 1993; Pesonen et al., 2003, Lahtinen et al., 2023), and presently covered by Phanerozoic sediments in its eastern and southeastern part (Nikishin et al., 1996; Raukas and Teedumäe, 1997; Šliaupa and Hoth, 2011). In the Fennoscandian Shield the rocks are Neoarchean to Proterozoic with ages becoming younger towards the SW reflecting plate tectonic amalgamation and crust-forming processes (Berthelsen, 1980; Gaál and Gorbatschev, 1987; Nironen, 1997; Berthelsen, 1992; Gee and Stephenson, 2006; Hölttä et al., 2006; Stephens and Weihed, 2013; Lahtinen et al., 2023). The most important crust-forming processes occurred in the Paleoproterozoic Svecofennian (ca. 1.92–1.77 Ga) (Lahtinen et al., 2023) and the Meso-Neoproterozoic Sveconorwegian (Grenvillian) (1.15–0.9 Ga) orogenies (Bingen et al., 2008). Late post-orogenic Rapakivi granite magmatism was extensive in the Mesoproterozoic producing large intrusions on the present erosion level in Finland, Russia and beneath the Baltic Sea (Rämö and Haapala, 2005). Mesoproterozoic sandstone and siltstone units occur in paleo-rifts onshore in Finland and offshore in the Bothnian Sea and Bothnian Bay (Floden et al., 1979; Winterhalter, 1972; Wannäs, 1989; Kohonen et al., 1993; Koistinen et al., 2001; Kohonen and Rämö, 2005).

The Sveconorwegian orogeny at 1.15–0.9 Ga (corresponding to the Grenville orogeny in North America) amalgamated the youngest Precambrian component to Baltica in the southwest (Bingen et al., 2008). The Sveconorwegian foreland sediments attained a thickness of several km and may have covered large areas in Sweden and Finland as indicated by titanite and zircon fission-track data in eastern Sweden (Larson et al., 1999). Exhumation of the Sveconorwegian foreland sediments and the subsequent Silurian-Devonian Caledonian orogeny and its foredeep sedimentation completely overprinted the Sveconorwegian record in the shield rocks. After the Sveconorwegian orogeny, Baltica was part of the Rodinia supercontinent (Li et al., 2008) and the subsequent Neoproterozoic geological evolution involved gradual peneplanation up to the end of the Precambrian (Kohonen and Rämö, 2005; Lidmar-Bergström, 1995) until the break-up of Rodinia at ca. 600 Ma (Torsvik and Cocks, 2005; Merdith et al., 2021). The long period of denudation facilitated the completion of the peneplain.

Remnants of Neoproterozoic and Phanerozoic orogenies surround Baltica, namely the Scandinavian Caledonides (490–390 Ma), Variscides (370–290 Ma), Uralides (320–250 Ma), Timanides (620–555 Ma) and Alps (65–2.5) Ma (Gee and Stephenson, 2006). All these have presumably produced far-field stress effects on Fennoscandia, but the nearest and most important is the Silurian – Devonian Caledonian orogeny (Gee, 1975, 2020, 2021; Roberts, 2003; Tuuling, 2019). In the Cenozoic, the shield area was affected by the uplift of the North Atlantic margin in the Paleocene (opening of the N Atlantic, 54 Ma, Mosar et al., 2002), and the Plio-Pleistocene northern hemisphere glaciations (Doré, 1992; Riis, 1996; Anell et al., 2009, Anell et al., 2010).

Intracratonic sedimentary basins in the Baltic Sea, Bothnian Sea and White Sea and the Ladoga and Onega paleo-rifts (Nikishin et al., 1996; Kohonen and Rämö, 2005) comprise mainly Mesoproterozoic and some Neoproterozoic sediments. The available geological evidence suggests that southern Finland was buried in the Mesoproterozoic with Jotnian sandstone and siltstone at ca. 1,500–1,100 Ma (Kohonen et al., 1993). Apparent lack of cover during 1,100–900 Ma (e.g., Hall et al., 2021) coincides with the late stages of the Sveconorwegian orogeny in

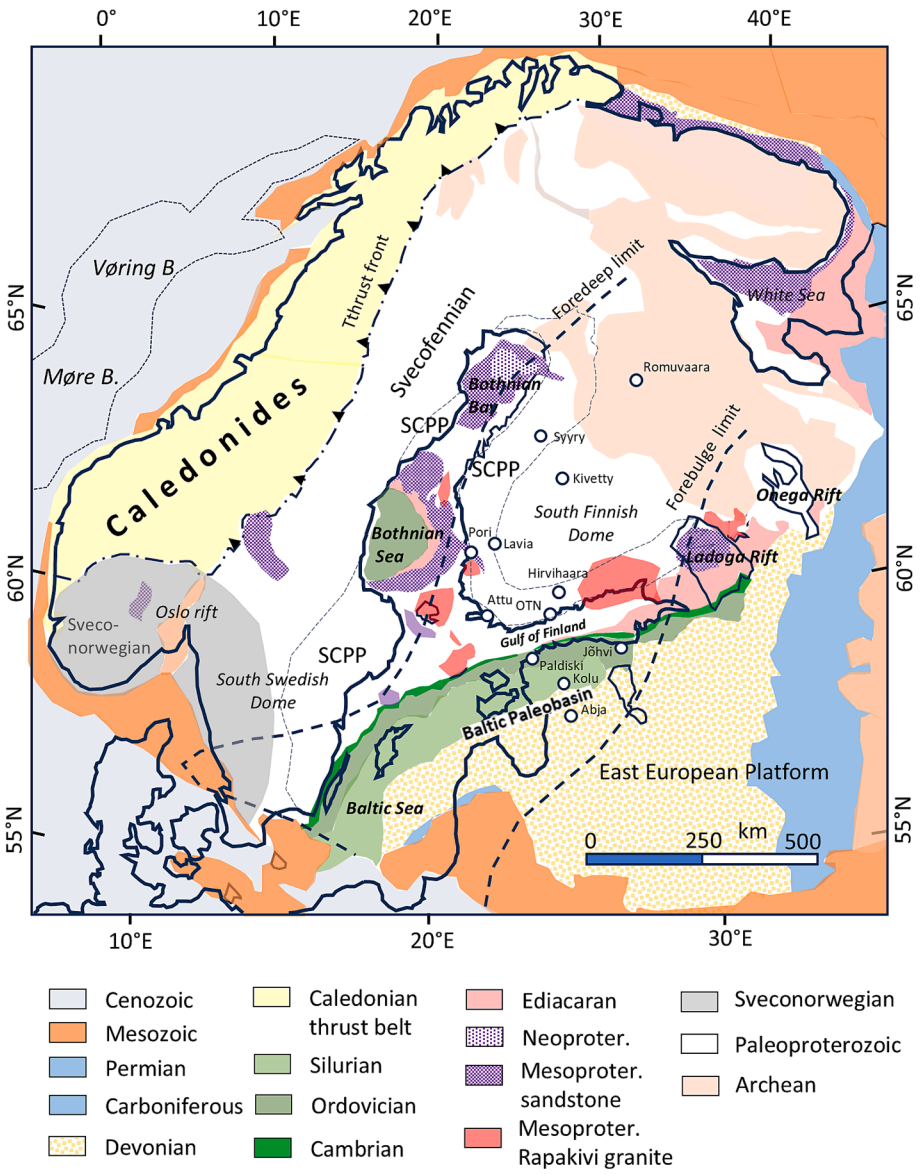


Fig. 1. Geological overview of Fennoscandia, the Baltic Paleobasin and surrounding sedimentary areas with locations of AFT samples indicated (see Table 1). SCPP, Sub-Cambrian Peneplain. The map is based on Andersen and Taylor, 1988; Koistinen, 1994; Samuelsson and Middleton, 1998; Bogdanova et al., 2006; Koistinen et al., 2001, Færseth, 2021; Hall et al., 2021, Gee (2021), Green et al. (2022). (For interpretation of the references to colour in this figure legend, the reader is referred to the web version of this article.)

southwestern Baltica and may reflect exhumation due to inversion of the Sveconorwegian foredeep basin (Larson et al., 1999). A thin cover of platform sediments was probably present in southern Finland in the Neoproterozoic. By the end of the Ediacaran Baltica was exhumed close to sea-level and the Sub-Cambrian peneplain (SCPP) was formed. The peneplain extended over most of Baltica. At present it outcrops in Fennoscandia and can be followed as an unconformity under sedimentary cover in the East European Platform (Nikishin et al.,1996; Lidmar-Bergström, 1996; Nielsen and Schovsbo, 2011; Šliaupa and Hoth, 2011; Petrov et al., 2016).

Phanerozoic sediments are not generally preserved in the shield, except in the Bothnian basin (Fig. 1) (Floden et al., 1979; Axberg, 1980; Winterhalter, 1972; Wannäs, 1989), in outliers onshore (e.g. Lauhanvuori, W Finland; Simonen and Kouvo, 1955; Tynni and Hokkanen, 1982; Söderman et al., 1983), in clastic dykes of Cambrian sandstone deposited in extensional dykes in SCPP basement (Bergman 1982; Friese et al., 2011), and in meteorite impact craters (Hall et al., 2021; Hietala et al., 2023). Phanerozoic impact craters are recorded in Cambrian and Ordovician target rocks, indicating that a thin platform and shallow marine sedimentary cover existed at the time of impacts, and the preserved crater fill sediments range up to Ordovician (Hall et al., 2021).

South of the Gulf of Finland, the geology is dominated by the sedimentary cover of the Paleo-Baltic basin. The basin covers the southeastern part of the present Baltic Sea basin and the western part of the East European Platform with extensive sedimentary cover continuing up to the Urals in the east. In northernmost Estonia, the thickness of Phanerozoic sediments overlying the Precambrian is 100–200 m. The sediments thicken towards the south and southeast and attain a thickness of about 700 m in northern Latvia. Further south, the basin deepens to 2,500 m and is finally truncated by the Trans-European Suture Zone, in the southern border of Baltica (Poprawa et al., 1999; Šliaupa and Hoth, 2011; Nielsen and Schovsbo, 2011; Gibbard and Lewin, 2016).

Sedimentary rocks in Estonia are unmetamorphosed and scarcely deformed (Raukas and Teedumäe, 1997; Kirsimäe et al., 2020). Ediacaran sediments (mostly sandstones and silty clays) unconformably overlie crystalline Precambrian basement rocks, and these, in turn, are

overlain by Cambrian terrigenous clays, silt and sandstone, Ordovician and Silurian shallow water marine carbonaceous sediments and Devonian sandstones and dolomarls. The succession has been continuous except for some minor breaks in the upper Cambrian and Ordovician–Silurian and Silurian – Devonian boundaries (Šliaupa and Hoth, 2011). Illite-smectite transition temperatures indicating maximum paleotemperature of 50–60 °C, are consistent with the uncompacted nature and thermally immature organic material of Lower Cambrian clay in Estonia. The corresponding burial depth in Estonia is estimated to have been less than 1 km (Kirsimäe et al., 2020).

Detrital U-Pb zircon data on Cambrian and Devonian sandstones in Estonia and Latvia indicate that their provenance was the Precambrian basement with ages ranging from Neoproterozoic to Archean, mainly from Baltica, but with a possible link to Avalonia (Põldvere et al. 2014). A change in provenance between Lower Cambrian stages 2 and 3 is also indicated (Isozaki et al, 2014). Ediacaran and Lower Cambrian stage 2 sandstones carry mainly 1,600 Ma zircons (corresponding to Mesoproterozoic Rapakivi granites in SE Finland), while Lower Cambrian stage 3 contain Neoproterozoic – Archean zircons suggesting a much wider circulation of detritus (Isozaki et al., 2014).

The development of the Baltic Sea basin began in the Ediacaran-Cambrian on a passive margin of Baltica (Nikishin et al., 1996; Šliaupa and Hoth, 2011; Gibbard and Levin, 2016). There are no sediments preserved between the Jotnian (Mesoproterozoic 1,300–1,400 Ma) and Ediacaran, suggesting a relatively stable plate tectonic setting of Baltica with gradual denudation and peneplanation. Basin development commenced with marine transgressions in the late Ediacaran and Early Cambrian (Šliaupa and Hoth, 2011). Ediacaran sediments comprise sandstones and conglomerates deposited in a shallow marine environment. The overlying Cambrian sediments are siliciclastic quartz sandstones, siltstones and shales with a total thickness of up to 100 m in Estonia and Latvia, and up to 500 m in northern Poland (Šliaupa and Hoth, 2011). In the Ordovician, the basin developed in a shallow marine environment with deposition of up to 250 m of marine carbonates and graptolitic shales (Bauert, 1993; Raukas and Teedumäe, 1997; Samuelsson and Middleton, 1998). In the Silurian, carbonates were deposited in shallow marine environments in Estonia and Latvia, while in deeper parts of the Baltic basin, graptolitic shale, marl, and limestone are typical (Šliaupa and Hoth, 2011). In the Devonian, the most important depocenter was in the west in the present Baltic Sea area and Sweden, apparently in the Caledonian foredeep basin (Buchardt and Nielsen, 1985; Samuelsson and Middleton, 1998; Tullborg et al., 1995; Larson and Tullborg, 1998; Larson et al., 1999; Gee, 2020, 2021). The preserved Devonian sediments are shallow marine sandstones and shales alternating with lagoon carbonates and marlstones. The Devonian siliciclastics represent foredeep sediments of the Caledonian orogeny (Plink-Björklund and Björklund, 1999; Põldvere et al. 2014). Onshore Sweden and Finland Devonian sediments are not preserved (Cederbom et al., 2000).

Several unconformities and paleic surfaces are preserved in the shield area. They range in age from Lower Proterozoic to Cenozoic (Lidmar-Bergström, 1996; Lidmar-Bergström and Näslund, 2002; Japsen et al., 2002, 2018; Hall et al. 2021). The best preserved are the sub-Cambrian peneplain (SCPP) and the undulating Mesozoic-Cenozoic hilly terrain (MCHT) surfaces in Finland and Sweden. The SCPP is represented by extensive flat landforms in coastal areas of Sweden and Finland (Söderman, 1985; Lidmar-Bergström 1996; Hall et al., 2021). In central-southern Finland the SCPP surface has been deformed into a domal shape with an amplitude of about 500 m between eastern Sweden and Lake Ladoga (Hall et al., 2021). In central Finland, the SCPP surface was later eroded by about 100–200 m when the hilly terrain landscape (MCHT) was formed in the Mesozoic – Cenozoic. It is also conceivable that the central Finland basement was exhumed already in the Devonian during the foreland bulge stage (section 5.3) and was then overlain by Devonian sediments until final exposure in the Cenozoic. In southern Sweden, the SCPP forms a domal shape like that in Finland, but it is surrounded by sedimentary blankets ranging from Cambrian to Quaternary (Japsen et al., 2002; Lidmar-Bergström et al, 2013). The occurrence of clastic dykes of Cambrian sandstone filling extensional fractures in the granitic basement indicate that peneplanation of Baltica was completed in the late Neoproterozoic (Bergman 1982; Friese et al., 2011) after several hundred million years of denudation (Kohonen and Rämö, 2005; Lidmar-Bergström, 1995). The presence of the SCPP is an important observation suggesting that during the Late Neoproterozoic and Cambrian the erosion surface was very close to the present one.

The MCHT surface developed over a long time in the Mesozoic and Cenozoic. It cannot be dated very accurately, and it never developed to a complete peneplain (Söderman, 1985; Lidmar-Bergström, 1995; Lidmar-Bergström and Näslund, 2002). In Sweden, the MCHT developed apparently in sub-Cretaceous time, as indicated by partly preserved Early to Late Cretaceous sedimentary cover (Lidmar-Bergström, 1995; Gilg et al., 2013). MCHT development continued in Finland in the Cenozoic as indicated by deep kaolinic weathering under humid and cool climatic conditions in the Paleocene-Eocene and/or the Late Oligocene – Middle Miocene (Gilg et al., 2013; Hall et al., 2024). In Finland, the MCHT is represented by the lake district in central Finland.

3. Materials, methods and fission track analysis

We use both published raw AFT data from seven boreholes in southern Finland (Green et al., 2022) and new data from four boreholes in Estonia. Drill core samples from the latter basement were analyzed at the University of Melbourne for AFT and modelled. Sample information is given in Table 1, and locations shown in Fig. 1. Sample metadata and detailed thermochronology analytical data can be accessed and interrogated geospatially in the EarthBank data platform (formerly AusGeochem, Boone et al., 2022; Boone et al., 2023): Doi-https://doi.org/10.58024/AGUM799F93C9.

Most samples analyzed were from the crystalline basement (granitic and metamorphic rocks) in Finland and Estonia. Sedimentary rocks were not included, except for a Mesoproterozoic sandstone in the Pori drill hole in Finland. In the shield the samples represent depth ranges from ground surface to about a depth of 1 km level, but at the OTN site in Finland, data was available up to a depth of 6 km. In Estonia, the samples are from the crystalline basement at depths of 198–750 m below ground surface and 20–580 m below the top of the basement (SCPP). Techniques and analysis of AFT data (ages, track lengths) of the samples from Finland were reported in Green et al. (2022). Mineral separations and AFT analyzes were carried out at the University of Melbourne following the protocol of Seiler et al. (2023). For further details see also Table S1 and Doi-https://doi.org/10.58024/AGUM799F93C9.

Time - temperature (t-T) histories were modelled using the HeFTy software (Ketcham, 2005; version 2.1.7) for forward and inverse modeling of LTT data. HeFTy applies a Monte Carlo search method for inversion and allows the setting of independent constraints on the t-T history. The annealing model of Ketcham et al. (2007) was applied in AFT inversion modeling, using D_{par} as the kinetic parameter for the Estonian samples and Cl concentrations (Green et al., 2022) for the Finnish samples. Track lengths were projected on to the crystallographic c-axis. In two cases, ^{252}Cf-tracks were implanted to increase the number of measurable confined track lengths (Table 1).

4. Results

4.1. Central ages and inverted time–temperature paths

Central ages and other information for the new results are given in Table 1. The central ages of the whole data set range from 2 Ma (OTN, 6 km depth) to 824 Ma (Jõhvi, 566 m). Most of the near surface samples (<500 m) have resided most of the Phanerozoic at temperatures < 60–70 °C. Values higher than that are probably due to hydrothermal effects (see 5.4 and 5.5).

Table 1
Estonia boreholes AFT data.

Sample no.	Site	Depth b. s. [m]	N_{grains}	N_s	ρ_s [10^5 cm^{-2}]	^{238}U [ppm ± 1σ]	Pooled age [Ma ± 1σ]	Central age [Ma ± 1σ]		N_{length}	Mean track length [μm ± se]		St.D. [μm]	D_{par} [μm]	Cl wt% average (range)
AFT-01	Paldiski	757	21	905	1.403E + 06	5.66 ± 6.03	515.3 ± 26.0	529.0	±	26.9	103	11.53	± 0.20	2.06	1.46 ± 0.12	0.007 (0.00–0.019)
AFT-03	Paldiski	198	20	1326	5.293E + 06	14.97 ± 5.36	734.4 ± 38.7	731.5	±	36.4	116	11.42	± 0.16	1.71	1.44 ± 0.07	0.021 (0.00–0.050)
AFT-04	Jõhvi	696	31	1988	4.071E + 06	11.68 ± 4.75	726.0 ± 24.5	723.3	±	24.3	107	11.34	± 0.16	1.66	1.68 ± 0.08	0.199 (0.101–0.438
AFT-05	Jõhvi	523	34	5029	5.759E + 06	17.72 ± 8.82	665.5 ± 25.7	699.9	±	23.5	137	11.70	± 0.15	1.71	1.66 ± 0.05	0.103 (0.066–0.152)
AFT-06	Jõhvi	567	31	4224	6.064E + 06	15.06 ± 4.90	819.2 ± 14.6	823.8	±	21.3	135	11.74	± 0.13	1.57	1.73 ± 0.06	0.162 (0.042–0.268)
AFT-07	Jõhvi	272	28	1938	6.450E + 06	23.06 ± 4.90	575.1 ± 26.6	574.9	±	26.0	157	10.99	± 0.16	1.98	1.51 ± 0.06	0.062 (0.00–0.172)
AFT-08	Kolu	448	25	2850	8.608E + 06	25.91 ± 11.71	718.2 ± 29.2	699.1	±	28.0	95	11.56	± 0.15	1.50	1.68 ± 0.12	0.168 (0.075–0.391)
AFT-09	Kolu	486	23	2118	6.261E + 06	17.55 ± 8.46	756.7 ± 38.5	763.0	±	36.4	98	11.27	± 0.18	1.74	1.59 ± 0.10	0.217 (0.102–0.385)
AFT-10	Abja	580	32	2256	8.877E + 06	26.81 ± 11.14	681.8 ± 29.2	687.6	±	28.0	54	11.76	± 0.22	1.63	1.82 ± 0.15	0.252 (0.131–0.491)

Notes: Analyses were performed on image sets captured by TrackWorks. Spontaneous track densities were measured on prismatic internal apatite surfaces after etching with 5 M HNO3 for 20 s at 20 °C. Track counts were obtained by automated counting in FastTracks using the 'coincidence mapping' technique of Gleadow et al. (2009) followed by manual inspection. Uranium concentrations of each grain were determined by LA-ICP-MS single spot analysis using a New Wave Nd:YAG Laser (λ = 213 nm with 5 Hz @ 50–55 % power, spot size = 30 μm) connected to an Agilent 7700x mass spectrometer. NIST612 was used as an internal LA-ICP-MS standard. Single grain and pooled ages were calculated according to Hasebe et al. (2004) (constants used: apatite density = 3.21 g/cm3, apatite R (0.5*10) = 7.17E-04 cm, apatite q (etch fact) = 0.93, λD = 1.55E-10 t-1, λf = 8.46E-17 t-1, Zeta = 2167). Central ages were estimated from single grain ages and errors according to the formulas given by Galbraith (2005, p.100) using the Newton-Raphson method. For sample AFT-01 and AFT-04, confined fission-track lengths were determined on a second polished mount that was exposed to a 252Cf fission source prior to acid etching to enhance the number of measurable confined track lengths (Donelick and Miller, 1991). Ns = number of spontaneous tracks counted; ρs = spontaneous track density; Dpar = long axis of track etch pit; Nlength = number of lengths measured; se = standard error.

In constructing the inverse models, we preferred simplicity and avoided creating unnecessary complexity which would not be geologically conceivable. Therefore, we applied only two tight constraints in the inversions, namely the SCPP and the present sample temperature. The other t-T boxes applied were relatively large (see Supplementary data) allowing a wide range of possible temperature histories to be tested by the software. Our method differs especially from the method applied in Green et al. (2022) where several cooling periods are fundamentally assumed to have occurred.

In the Monte Carlo search 50,000 to one million (in most cases 200,000) t-T paths per model were tested. All inverse models (see supplementary data) are single sample inversions. Modeling resulted typically in 300–4,000 statistically 'acceptable' and 10–500 'good' models (goodness of fit values above 0.05 and 0.5, respectively). For the definition of acceptable and good models, see Ketcham (2005). As all samples (excluding the deeper OTN samples) are within one km of the SCPP surface, it was used as a constraint in all models for inverting the t-T history. Surface temperature was assumed to have been 20 ± 10 °C at 575–625 Ma, adjusted for the present T-z value depending on the depth of the sample and present geothermal gradient (10–15 K/km).

An example of the inversion results is shown in Fig. 2. Time-temperature histories of near-surface (<500 m) samples inverted are remarkably consistent as shown in the compilation of t-T histories (Fig. 3). The results suggest heating after the SCPP stage in the Cambrian up to end Carboniferous (300 Ma), followed by cooling from the Early Permian to present. Inverted t-T paths for 500–1000 m depth are analogous, but the Finnish samples tend to show paleotemperature maxima at much older ages (Fig. 4). We attribute these effects to hydrothermal alteration (see 5.5).

The typical partial annealing zone (PAZ) of apatite fission tracks is ~ 60–110 °C (Gleadow and Duddy, 1981). Due to this inherent characteristic of the AFT method, it does not usually provide information on paleotemperatures ≤ 60 °C or ≥ 110 °C. Our results suggest the present bedrock surface in Finland and the uppermost basement in Estonia has not experienced temperatures above ~ 60–80 °C in the Neoproterozoic and Phanerozoic. This is also expressed in the central ages which are relatively old (Table 1, and Green et al., 2022).

4.2. Average erosion rate during last 300 Ma

Based on the assumption that heating and cooling recorded in the models was related principally to sedimentary burial and denudation, the present results allow estimation of the thickness of the section removed over the last ~ 300 Ma. We assume that the sedimentary section removed comprised mainly Devonian and Carboniferous clastic sediments (shale and/or sandstone). In Finland these were underlain by a thin or discontinuous veneer of Ediacaran-Silurian sediments. Some Precambrian crystalline rock was probably also eroded in the Mesozoic – Cenozoic, but its resistance to erosion would have been much higher than the sediments.

The present heat flow density measured in < 1 km deep holes in southern Finland and Estonia is 30–69 mWm^{-2} (Kukkonen and Jõeleht, 1996; Veikkolainen and Kukkonen, 2019). These values are influenced by the conductive paleoclimatic effect of Plio-Pleistocene glaciations and Holocene climatic variations. For a steady-state paleoclimatically corrected heat flow density a value of 60 mWm^{-2} is applied (Kukkonen and Jõeleht, 2003). The decrease in paleotemperature since the early Permian has been about 50 °C (Fig. 3).

The paleotemperature change recorded by AFT data since the Permian (Fig. 3) consists of two components. First, there is a paleoenvironmental change in surface temperature since the Permian due to climatic and paleogeographic factors, such as the paleolatitude drift of Baltica, and second, a cooling effect due to erosion. Surface temperature in Estonia is estimated to have been ca. 15–20 °C higher than present during the Carboniferous – Permian (Kirsimäe et al., 2020). Similar conditions have presumably prevailed in Finland. Considering the

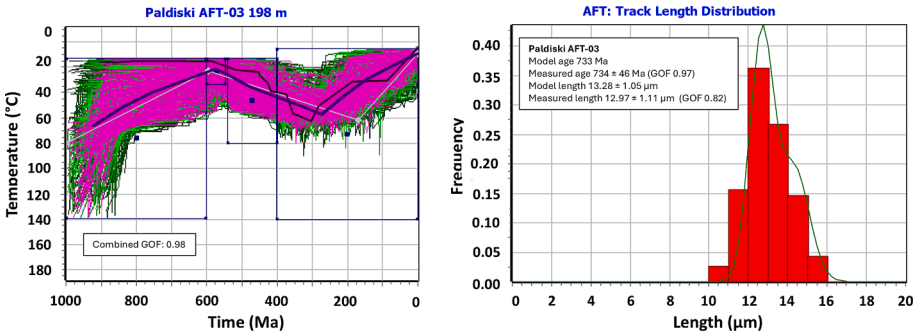


Fig. 2. Example of typical inversion results of near-surface samples, Sample AFT-03 (Paldiski, Estonia). On the left inversion results calculated with HeFTy v. 2.1.7. Blue boxes show applied t-T constraints for each labeled interval. The thin black line is the best fit path, the thick black line is the weighted mean of statistically good and acceptable paths. On the right, the analyzed and modelled track lengths are shown. The modeled track length distribution (thin solid line) is for the best fit model, showing also central age and GOF (goodness of fit). Central ages and mean fission track lengths are given for the experimental data (Table 1) and the inverse model. Similar results for all inversions are given in the Supplementary data. (For interpretation of the references to colour in this figure legend, the reader is referred to the web version of this article.)

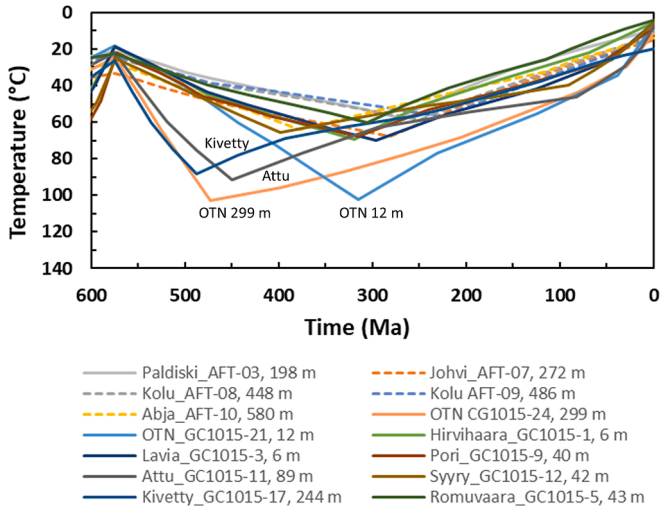


Fig. 3. Weighted mean t-T histories inverted for the Finnish (solid lines) and Estonian (dashed lines) samples showing weighted mean curves of HeFTy inversions of the samples at borehole depths < 500 m. The cases for OTN, Kivetty and Attu differing from the general trend are discussed in detail in sections 5.4 and 5.5.

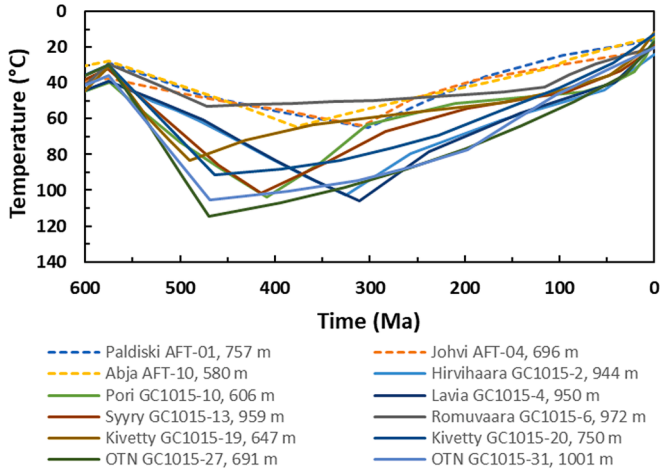


Fig. 4. Weighted mean t-T histories inverted for the Finnish (solid lines) and Estonian (dashed lines) samples showing weighted mean curves of HeFTy inversions of samples at borehole depths 500 – 1000 m.

paleoenvironmental change the remaining cooling effect due to erosion amounts to ~ 30–35 °C. Typical ranges of porosities and thermal conductivities of Devonian siliciclastics are 15–30 % and 1.7–3 $Wm^{-1}K^{-1}$, respectively. The majority of the data show saturated rock conductivities in the range of 2.0–2.5 $Wm^{-1}K^{-1}$ (Jõeleht and Kukkonen, 2002). With a matrix conductivity of 3.5 $Wm^{-1}K^{-1}$, typical for micas, feldspars, clays, and some quartz, and thermal conductivity of the pore water as 0.6 $Wm^{-1}K^{-1}$, the saturated rock conductivity estimated with a geometric average model would be 2.06–2.69 $Wm^{-1}K^{-1}$ (porosity 30–15 %). This yields an estimate of the removed section as ~ 1.6–1.0 km in Finland and ~ 0.5 km in Estonia, and an average erosion rate for the last 300 Ma as 4.3 ± 1 m/Ma. The value is higher than the estimate of 2.5 m/Ma proposed by Hall et al (2021) for southern Finland, which was based on 'tiered unconformities' for the last 1 Ga.

5. Discussion

5.1. General

AFT ages of near surface/near SCPP samples in Estonia are relatively old (515–819 Ma) and younger in S and SW Finland (500–215 Ma). The mean track lengths (ca. 11.0–11.75 µm) are relatively short compared to outcrop samples in many parts of the world, suggesting long residence under mild annealing conditions. In central and eastern Finland, the ages are older (up to 790 Ma) and comparable to those in Estonia. These results are in line with the AFT age data compilation of southern and central Finland by Kohn et al. (2009). AFT ages in Fennoscandia are very old, among the oldest in the world (Hendriks et al., 2007; Kohn et al., 2009; Kohn and Gleadow, 2019), indicating low paleotemperatures since the Neoproterozoic.

The inversion models reveal consistent t-T patterns for Finland and Estonia (Fig. 3), suggesting heating and burial from Cambrian to early Permian (ca. 300 Ma), and monotonous cooling and exhumation thereafter. The unroofing is also supported by inversions without the assumption of the SCPP (not shown). It should be noted that the paleotemperature maximum and its timing cannot be determined very accurately. The maximum is not always well defined and may well have occurred some 50 Ma earlier or later, and not necessarily coevally across the area. The cooling rate however was relatively uniform, although more rapid Cenozoic cooling is suggested by some inversions (see Supplementary data), but this is most probably an artefact due to the inability of the applied annealing model to handle very low temperature (<40 °C) annealing of fission tracks (Ketcham et al., 2007). Further, the inverted t-T histories are naturally strongly influenced by the applied SCPP constraint, and there is no extractable thermal history before the Cambrian, although some of the AFT ages are Neoproterozoic.

Our inverse modeling results differ essentially from the t-T histories recently suggested by Green et al. (2022) for the same Finnish samples. Their inverse algorithm assumes several cooling periods in the geological past of the samples. Unfortunately, we cannot find the method geologically feasible, at least not in the Fennoscandian case. Inverse modeling is ambiguous, and therefore we prefer to keep it as simple as the geological data suggests.

The present results show that AFT data provide relevant information on the thermal history of this ancient bedrock area, although the samples have experienced paleotemperatures close to or slightly below the partial annealing temperatures.

In a conductive heat transfer regime, the AFT ages should decrease with increasing sample depth. Deviations from this may be due to present or ancient fluid flow, tectonics or changes in conductive heat flow. In the present data some vertical variations of AFT ages (e.g., OTN) suggest ancient non-conductive heat transfer resulting in a scatter of AFT ages. We attribute this apparent deviation to a Devonian hydrothermal effect (see 5.5).

5.2. How the present Fennoscandian shield was exhumed

AFT data suggest there was a thickening of sedimentary cover in Finland and Estonia during Cambrian – Carboniferous time. Thus, Finland was most probably the northern part of the Baltic paleobasin and in the foredeep/forebulge area of the Caledonian orogeny (Fig. 1). Ediacaran and Lower Cambrian (up to LC2) sediments in Estonia have a provenance consistent with the basement in central and southern Fennoscandian shield, i.e., dominantly zircons of Rapakivi age (1,650–1,500 Ma) with smaller Paleoproterozoic (Svecofennian) and Neoarchean (Kola – Karelia) components (Isozaki et al., 2014). From Lower Cambrian (LC3) to Devonian detrital zircons yield ages ranging from Archean to Middle Proterozoic as in LC2, but a Neoproterozoic source is added. A simple interpretation of the detrital U-Pb zircon data would require that the Finnish area was deeply eroded during the Cambrian – Devonian and produced the sediments in the present Paleo-Baltic basin.

However, detrital zircon data is not a simple story of'from source directly to deposition'. Instead, multiple cycling of detritus from the Archean to Devonian must have been involved. Kristoffersen et al. (2014) studied the detrital zircons of Ordovician – Carboniferous sediments in the Oslo Rift (ca. 300 Ma) (Fig. 1) and noted that the detrital material comprises all known ages of rocks in Fennoscandia. It is therefore not possible to delineate the provenances of the sediments due to multiple craton-wide cycling of detritus. This is the intrinsic problem of using zircon as a tracer-mineral in 'source to sink' sedimentary provenance studies. It is quite feasible that Ediacaran and Cambrian sediments in Baltica at large (and not only in Estonia) already contained a component of zircon ages ranging from Archean to Neoproterozoic. Thus, we cannot use detrital zircon ages from sedimentary rocks as compelling evidence for an immediate provenance for a particular sediment.

It is conceivable that the sedimentary cover in Finland comprised a thin (<1.5 km) unit of sediments deposited in the Ediacaran-Carboniferous. Such a thin layer of poorly consolidated rocks would have been much more susceptible to erosion than the underlying crystalline basement. Resolution of the AFT data and low paleotemperatures do not allow for deducing any details of the burial history, i.e., the marine stages in the Ordovician – Silurian, the foredeep sedimentation in the Devonian and the sedimentation in the Paleo-Baltic basin and on the fore bulge up to end of Carboniferous. These are all included, without differentiation, in a monotonous warming trend in the AFT inversions (Figs. 2–4).

Further, the AFT data suggest a gradual, monotonous unroofing of the sedimentary cover in Finland and thinning of the sediments in Estonia since the early Permian. In the following, we present a model for the geological history which honors the AFT data. The model is closely related to the Caledonian orogeny and the dynamic development of its foredeep basin and forebulge uplift, and the related periods of subsidence, uplift, and erosion.

5.3. Modeling the Phanerozoic thermal history of Fennoscandia

Correlation of AFT results and major geological events is presented in Fig. 5. In the late Neoproterozoic, Fennoscandia was a part of the supercontinent Rodinia comprising Laurentia and Baltica. Separation of Laurentia and Baltica took place at about 600 Ma or slightly thereafter (Merdith et al, 2021; Torsvik and Cocks, 2005). The lithospheric extension is indicated by e.g., the emplacement of deep-derived carbonatitic and kimberlitic magmas, namely the Fen alkaline complex in Norway at 539 Ma (Andersen and Taylor, 1988), Alnö carbonatite complex in Sweden at 584 Ma (Meert et al., 2007) and kimberlites in Finland at 600 Ma (O'Brien et al., 2005). After continental break-up an oceanic basin, the Iapetus Ocean, developed between Baltica and Laurentia. The ocean existed for about 150 Ma (Roberts, 2003; Gee, 1975, 2020, 2021) before closure of the basin during the Caledonian orogeny.

Closure of the Iapetus Ocean between Laurentia and Baltica took place from the Late Cambrian to Late Ordovician, with subduction and tectonothermal activity on both margins of the oceanic lithosphere, accretion of arcs and thrusting of ophiolites onto Baltica (Gee, 2020, 2021). Laurentia-Baltica continent–continent collision (the Caledonian Scandian orogeny) took place from the Late Silurian to early Devonian, culminating at 425 ± 25 Ma (Dunlap and Fossen, 1998; Gee, 2020, 2021). Slices of Baltica were thrust under Laurentia with Cambrian alum shales serving as thrusting surfaces (Juhojuntti et al., 2001; Gee et al., 2010; Juhlin et al., 2019; Gee, 2021). Before break-up in the Cenozoic, the resulting Caledonian mountain range, was about 1,000 km wide and 3,000 km long. At least 300 km of shortening has been interpreted from overthrust sheets. The original thrust sheet probably extended more than 100 km to the SE of the present outcrop (Fig. 1) of the Caledonian front (Morley, 1986). Temperature of the basal thrust may have reached ca. 500 °C at 1.2 GPa (Fauconnier et al., 2014).

Extensional collapse of the orogen began shortly before 400 Ma with reactivation of the basal decollement of the orogenic wedge as a low-angle normal shear directed westward (Andersen et al., 1991; Dunlap and Fossen, 1998). It resulted in fast cooling and large-scale exhumation of the thrust belt in the Devonian. After orogenic collapse relative tectonic stability is assumed to have prevailed until formation of the Oslo rift at ca. 300 Ma (Dunlap and Fossen, 1998).

The preserved autochthon in the central Scandes has about 2 km of Ediacaran – Middle Silurian sediments (Gee, 2020, 2021) corresponding to those in the Paleo-Baltic basin. Coarse Devonian Old Red molasse deposits are preserved in Norway in small fault-limited extensional basins formed during the orogenic collapse (Seranne and Seguret, 1987; Fossen and Dunlap, 1998; Cederbom et al. 2000). In Sweden and Finland, no Devonian deposits are known (Cederbom et al., 2000; Kohonen and Rämö, 2005). Devonian sediments in the Paleo-Baltic basin are less coarse, mature siliciclastic quartz arenitic sandstone and shale, implying more efficient sorting and longer transport distances. The characteristics and depositional environment of Devonian sediments in the Paleo-Baltic basin indicate deposition in the foredeep basin stage of the Caledonian orogeny (Plink-Björklund and Björklund, 1999; Põldvere et al., 2014), analogous to the Old Red sediments occurring widely in areas of Caledonian orogeny in Europe, Greenland and North America.

An important factor in modeling the AFT data and the sedimentary history of Fennoscandia is the lithospheric flexure produced by the Caledonian thrust belt. The crust was thickened by a factor of about two in the orogenic front, raising mountains up to elevations of ~ 7–8 km (Samuelsson and Middleton, 1998; Cederbom et al., 2000; Gee, 2020, 2021, Gee et al., 2010) resulting in a significant lithospheric flexure. The modern continental lithosphere comprises a viscous deep layer overlain by an elastic layer with a thickness of about 80–100 km (Cloetingh,

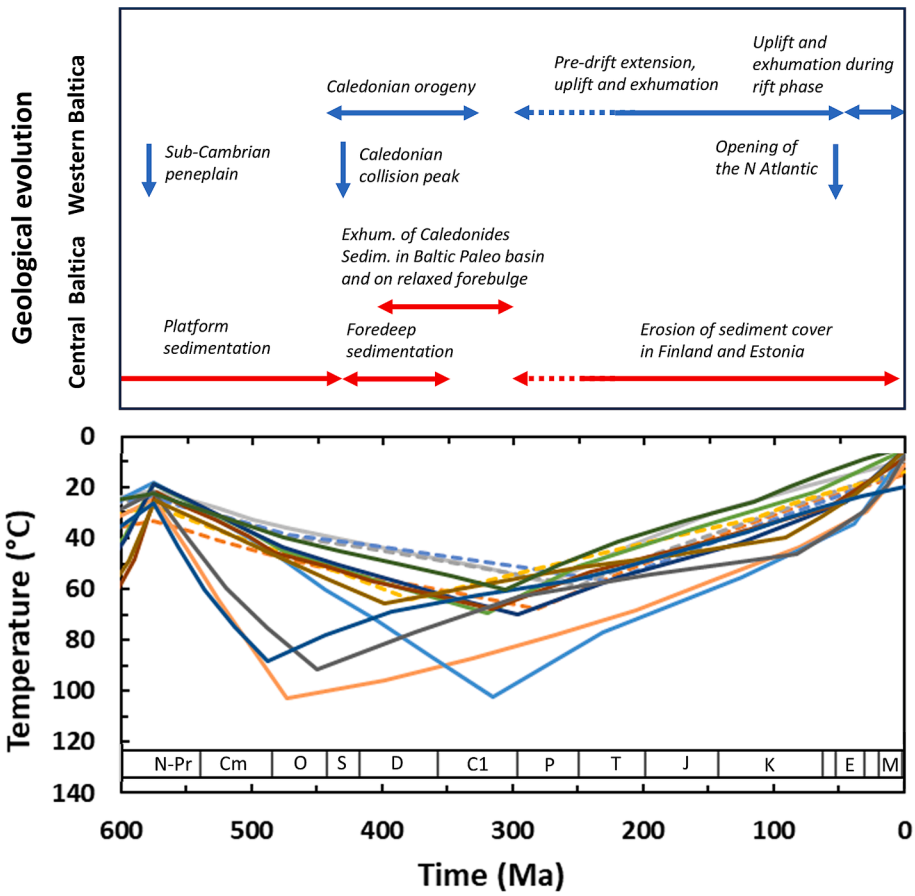


Fig. 5. Correlation of AFT results in Estonia and Finland (lower panel, near-surface samples, Fig. 3) and the geological history of the Caledonian thrust belt and sedimentation history in Fennoscandia (upper panel, see text for details).

1988; Ranalli, 1995). Similar conditions prevailed conceivably in Baltica in the Devonian. Under such an orogenic load the lithosphere was flexed, and a foredeep basin up to 6.5 km deep and extending 500 km from the thrust belt was formed (Fig. 1) (Samuelsson and Middleton, 1998). Beyond the foredeep, a forebulge 500 m high and 600 km wide was uplifted. The lithospheric flexure can be modeled with a line load model (Turcotte and Schubert, 2014). Further, using the principle of superposition we can add the effect of forebulge erosion to the model. Assuming the bulge is eroded by 400 m, i.e., there is an equal uplift simulated by an upward directed line load, the complete shape of the foredeep basin and forebulge uplift is modeled in Fig. 6. The elevation profile is in good agreement with the available evidence of the situation in the Devonian.

The foredeep basin was at its deepest next to the thrust belt but shallowed quickly with increasing distance from the belt. The foredeep width was limited on the distal side by the forebulge. After the orogenic collapse and rapid exhumation, the general topography nevertheless remained high, perhaps of the order of 1.5 km up to the end Carboniferous (Dunlap and Fossen, 1998; Fossen and Dunlap, 1998). The foredeep flexure would still have been of the order of 1–2 km at this time.

Elastic flexure of the lithosphere under an orogenic load is a very dynamic phenomenon, and as soon as the load is reduced by denudation of the mountains, the foredeep basin experiences uplift (inversion), and the basin sediments are eroded (Heller et al., 1988; DeCelles, 2012). Simultaneously, the forebulge correspondingly subsides, and may receive sediments from the eroding foredeep basin. The foredeep sediments may therefore be reworked and circulated within the basin between the thrust belt and the forebulge. Depending on sea level changes, erosion of the forebulge can also take place.

Numerical flexure modeling by Samuelsson and Middleton (1998) suggests that the Caledonian foredeep basin was at maximum about 6.5 km deep in western Sweden, but less than 1 km in eastern Sweden and in the Baltic and Bothnian Seas. The forebulge covered areas in Finland, the present Baltic Sea area and western part of the Baltic paleobasin in Estonia (Fig. 1). In Estonia a mild inversion of the paleobasin took place.

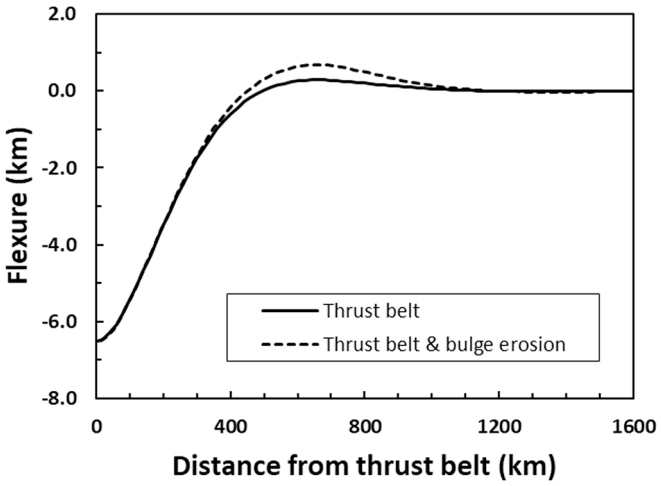


Fig. 6. Two-dimensional analytical modeling of the elastic lithospheric flexure under a line load. Solid line: Flexure of the lithosphere due to the thrust belt; dashed line: Flexure due to thrust belt and 400 m of erosion of the forebulge (Turcotte and Schubert, 2014, eq. 3.132). Applied lithospheric elastic properties: Young's modulus 70 GPa, Poisson ratio 0.25, flexural rigidity $3.82 \cdot 10^{24}$ Nm, effective elastic thickness 85 km.

The elastic lithospheric flexure model predicts strong horizontal variation in the sediment burial depth and paleotemperatures, in agreement with the AFT data on crystalline rocks and vitrinite reflectance data on Cambrian alum shales in Sweden (Samuelsson and Middleton, 1998; Tullborg et al., 1995; Larson and Tullborg, 1998; Larson et al., 1999; Cederbom et al., 2000; Schulz et al., 2021).

The height of the Caledonides topography following orogenic collapse is an important problem for interpreting the LTT data. K-feldspar ^{40}Ar-^{39}Ar and apatite and zircon fission track age data from southern Norway suggest rapid cooling of the Caledonides following the orogenic peak at about 425 Ma (Dunlap and Fossen, 1998; Fossen and Dunlap, 1998; Walsh et al., 2013). Orogenic collapse at about 400 Ma resulted in rapid exhumation of the thrust belt (Fig. 5), with more stable tectonic conditions prevailing subsequently up to 330–300 Ma. Thereafter, relatively rapid cooling of about 80 °C took place in the Permian at 300–250 Ma. An estimate of the corresponding thickness of denuded rock is 3 ± 1 km (Dunlap and Fossen, 1998). At the same time, the South Norwegian topography would have remained at about the 1.5 km level due to isostatic compensation. This is supported by paleogeographic reconstructions based on drilling and seismic data showing that up to the time of Late Jurassic rifting the area between Norway and Greenland was dominated by an emergent land mass separated by deep basins presently located in onshore East Greenland and offshore Mid Norway (Færseth, 2021). The long-term preservation of high topography is also indicated by the accumulation of large thicknesses of Triassic and Jurassic sediments in the North Sea (Møre and Vøring Basins, Fig. 1) and the Norwegian Sea (Steel, 1993; Müller et al, 2005).

The onset of cooling and uplift in Fennoscandia in Finland and Estonia at 250–300 Ma implied by the AFT data (Fig. 5) is coeval with cooling data of the Caledonides in the Carboniferous-Permian (Dunlap and Fossen 1998; Hestnes et al., 2024) and pre-drift extension of the present passive margin in W Norway (Mosar et al., 2002). This suggests a common craton-wide mechanism. We postulate that the lithosphere beneath the Caledonian thrust belt was thinned by convective thinning of the mantle part of the lithosphere triggered by extension starting from 250–300 Ma.

Although the Caledonian orogeny had collapsed at about 400 Ma, the lithosphere of the Caledonian thrust belt was still thick and warm due to radiogenic heating in the thickened lithosphere since the 425 Ma collision. Similar post-orogenic heating continuing up to 200 Ma after an orogenic peak has been modelled for the Paleoproterozoic Svecofennian orogenies in Finland (Kukkonen et al., 2008, Kukkonen and Lauri, 2009). The thickened and still warm thrust belt, several hundred km wide, was weaker rheologically than the surroundings due to elevated temperature. Therefore, when extension became possible in northern Europe in the final stages of the amalgamation of Pangea and the Variscan orogeny at about 300–250 Ma (Mosar et al., 2002), the strain was inevitably localized in the warm post-orogenic Caledonian lithosphere. Plate tectonic reconstructions of the North Atlantic suggest that extension and the making of the present passive margin in western Norway started at latest in the Late Permian (Mosar et al., 2002). Early extension of the Fennoscandian lithosphere is indicated by the formation of the Oslo rift at ca. 300 Ma (Larsen et al., 2008), and emplacement of dolerites in southern Sweden (and Germany) at 300–310 Ma (Timmerman et al., 2009; Obst et al., 2004). Contact metamorphic data on shales and carbonates in the Oslo rift indicate that the sedimentary sequence was $>$ 3.5 km thick at the time of the syenite intrusions (Aldridge, 1984; Svensen and Jamtveit, 1998).

Paleomagnetic fitting of polar wander paths of Fennoscandia and North America suggest about 450 km of pre-drift extension of the lithosphere in Mid Norway at least from about 214 Ma in the Triassic up to Mid-Jurassic (ca. 170 Ma) (Torsvik et al., 2001). The timing of extension onset is constrained by the availability of reliable magnetic paleopoles in the Triassic – Late Permian. Thus, extension of the Baltica lithosphere began well before the final stages of the opening of the North Atlantic basin in the Cretaceous – Paleogene (ca. 54 Ma; Mosar et al., 2002). The pre-drift extension provided a mechanism to accommodate the North Europe and Greenland lithospheres in the rotation of plates (Torsvik et al., 2001; Mosar et al., 2002).

Extension of the lithosphere generates either subsidence or uplift depending on changes in the buoyancy of the plate (Lachenbruch and Morgan, 1990; Esedo et al., 2012). Uplift takes place if the lithospheric mantle is thinned more than the crust, and in the opposite case, subsidence follows. The present lithospheric mantle in southern Norway is about 100 km thick, and about 200 km in the shield area to the east (Medhus et al., 2012; Plomerová and Babuška, 2010; Weidle et al., 2010; Maupin, 2011). We cannot say with certainty whether the present upper mantle architecture was achieved in the final break-up of the lithosphere in the Cretaceous – Paleogene or already during pre-drift time in the Permian – Triassic (Rohrman et al., 2002). Nevertheless, extension-stimulated uplift provides a plausible mechanism for explaining the geological evolution of the Caledonides and Fennoscandia in the Permian – Cretaceous. Thinning of the mantle lithosphere most probably began in the Permian as a result of convective delamination (Platt and England, 1993) of the mantle lithosphere under the warm Caledonian thrust belt. Thinning of the mantle lithosphere by a factor of two implies a total uplift of 1–2 km (Esedo et al., 2012). Thus, mantle lithosphere thinning enabled a rejuvenation of the Caledonian topography from the Late Carboniferous. Uplift occurred mostly in the former thrust belt, but flexure and tilting also affected the whole Fennoscandia and resulted in gradual thinning of sediments in Estonia and excavation of the Precambrian bedrock in Finland.

Other models have been proposed for the topographic evolution of western Fennoscandia. One, the ICE ('Isostasy-Climate-Erosion') model (Nielsen et al, 2009a,Nielsen et al., 2009b)suggests protracted post-Devonian erosion of the Caledonides facilitated by isostatic compensation and accelerated cold-climate driven erosion in the Cenozoic. On the other hand, geomorphology-based models suggest cyclic uplifts and denudation (Lidmar-Bergström et al., 2000; Fjellanger and Etzelmüller, 2003; Lidmar-Bergström and Bonow, 2009; Japsen et al., 2018; Japsen and Chalmers, 2022; Green et al., 2022) (see section 5.6).

Break-up of Greenland and Norway and opening of the North Atlantic took place in the Paleogene at ca. 54 Ma (Mosar et al., 2002; Torsvik and Cocks, 2005), presumably along a Caledonian rheologically weak suture zone. After break-up, mid-ocean spreading caused a shift in extension to the oceanic lithosphere. Uplift of the separating continental blocks was accelerated after break-up as the mechanical connection between them was lost. The development of the oceanic margin (Færseth, 2021) further thinned the mantle part of the continental lithosphere. Elastic flexure models suggest that the flexing force is doubled after the break-up (Turcotte and Schubert, 2014). Thus, continued, perhaps even faster uplift became possible in the Cenozoic during the drift phase. The uplift generated tilting of the lithosphere towards the southeast. Estimated values of Paleogene uplift are 600–1200 m in Norway and 400 − <200 m in Finland. Neogene uplift estimates are 500–1000 m in Norway and $<$ 500 m in Finland (Anell et al., 2009). These estimates are dependent on the factors assumed to be responsible for the uplift, and are thus debated in the literature (Nielsen et al., 2009a,b; Lidmar-Bergström and Bonow, 2009; Anell et al., 2010).

The cooling history indicated by the AFT data agrees with the above geological model (Fig. 5). All surface/near surface sample inversions suggest that most of the samples have resided at temperatures below the apatite PAZ since the end of the Carboniferous. Exceptions to this are most probably due to a mild hydrothermal effect (see 5.5.). The sedimentary cover was at its maximum thickness of $<$ 1.5 km at about 250–300 Ma during the Late Carboniferous – Early Permian. Due to a small depth of burial, we consider the sediments remained porous, were poorly consolidated and ranged in age from Neoproterozoic to Carboniferous, with Devonian shales and sandstones being an important component.

The presence of a thin sedimentary cover in Finland during Cambrian − Carboniferous time is supported by impact crater data. Twelve impact

craters are known in Finland, with diameters ranging from 1.5 to 23 km, and ages from Cretaceous to Proterozoic (Abels et al., 2002; Hall et al., 2021). Impact craters have characteristic excavation depth/diameter ratios, with the depth being considerably smaller than the crater diameter (Melosh, 1989; Masaitis, 2005; Wünnemann and Ivanov, 2003; Puura and Plado, 2005; Degeai and Peulvast, 2006). For instance, in simple craters with no central uplift the ratio is about 0.05, and in complex craters even smaller. In cases where there has been a sedimentary cover thicker than the depth of excavation of a given crater diameter, no impact scar is produced in the basement that could be recognized following erosion of the sediments. Thus, impact craters can be used as proxies for the approximate depth of burial at time of impact.

In Finland no impact craters are known in the interval 510–245 Ma (Hall et al., 2021), supporting the indicated increase in burial depth by the AFT results (Figs. 3 and 5). Before this period there had been three impacts in the Mesoproterozoic and six impacts in the Cambrian and Neoproterozoic between 520–710 Ma. In Estonia, the Cambrian Neugrund crater (diameter 8 km) and the Ordovician Kärdla crater (diameter 4 km) are dated as to have impacted at 535 Ma and 455 Ma, respectively, into a shallow marine basin (Suuroja and Suuroja, 2002; Puura and Plado, 2005). The next known impacts in Finland occurred in the Triassic at about 250 Ma (Karikkoselkä) and 231 Ma (Paasselkä). Hall et al. (2021) suggest that the lack of craters during the 'silent' period 510–245 Ma can be explained by a thin, ca. 1 km thick sedimentary cover. Further, the implied thinning of sediment cover in the Jurassic and Cretaceous agrees with the presence of the Lappajärvi (23 km, 79 Ma) and Suvasvesi (3.5 km, 85 Ma) craters. Otherwise, they would not have been preserved and our AFT data support these observations.

Removal of the sedimentary cover in Finland and thinning of the cover in Estonia took place in the Mesozoic and Cenozoic. The SCPP surface was folded in the Caledonian orogeny into a domal shape (Fig. 6), although probably relaxed to some extent in late- and post-orogenic time. It was gradually dissected by an erosion surface in Finland and Sweden, the MCHT surface, which is presently about 100 m below the extrapolated SCPP domal surface in southern-central Finland (Hall et al., 2021). As reviewed above (section 2) the development of the MCHT surface took about 200 Ma starting in the Triassic and concluding in the Miocene. Deep weathering under humid climates in the Mesozoic and Cenozoic is documented by kaolin deposits in Finland and Sweden (Söderman, 1985; Gilg et al., 2013), which have been preserved in tectonically controlled valley depressions, and not completely removed by Plio-Pleistocene glaciations. As the craton-covering sediments were conceivably porous and poorly consolidated due to shallow burial (section 4.2), Mesozoic – Cenozoic uplift and erosion removed the mechanically weak sediments down to the Precambrian crystalline basement.

Recently Hestnes et al. (2024) reported novel AFT and (U-Th)/He data on a 1.8 km high sample elevation transect in Nordfjord, southern Norway, and remodeled another 1.9 km high elevation transect in Jotunheimen using data by Green et al. (2022). The best fitting models of Hestnes et al. (2024) suggest that following Caledonian orogenic collapse, surface rocks presently outcropping at high altitude experienced rapid cooling and exhumation (about 120 m/Ma) up to end Permian, a much slower cooling (6 m/Ma) from the Triassic to Late Cretaceous, and finally an increased rate (40 m/Ma) from the Late Cretaceous to present. The cooling pattern from our AFT data in Estonia and Finland agrees with the monotonic slow Triassic – Present cooling trend of Hestnes et al. (2024). Moreover, their best-fit cooling history agrees well with the post-collapse development expected from our pre-drift extension and rift extension model above.

5.4. Age vs. depth in the AFT boreholes

Assuming the heat transfer in the crust has been conductive, the fission track ages of the samples are expected to decrease with increasing depth and temperature. It requires there has been no heat transfer by groundwater flow (ancient or present), recent tectono-thermal activity, or changes in the deep conductive heat flow (Duddy et al., 1994; Braun et al, 2006). Central ages of the studied boreholes vs. depth are plotted in Fig. 7. Deviation from a monotonous decrease of age with depth and higher maximum paleotemperatures (Fig. 3) are seen in OTN, Kivetty, Attu and Jõhvi boreholes.

Available petrological evidence shows that mild hydrothermal alteration has occurred at the OTN site at 0–300 m depth with formation of sericite, albite and hematite (Kuusirati and Toropainen, 2015), as well as much higher porosities (up to 6 %) than typical for intact crystalline rocks. The general trend of ages with depth seems to be locally disturbed at several depths to about 4 km level (Fig. 7). During drilling the OTN-1 and OTN-2 wells encountered a 400 m thick inclined zone of fractured and weak rock at 5 km level (Heikkinen et al., 2021; Kukkonen et al., 2023). The scatter of AFT ages with depth may be attributed to these mild hydrothermal effects.

The Kivetty data show no decrease of age in the uppermost 500 m (Fig. 7). Present heat flow in the borehole is quite low, 35.6 mWm^{-2} with a gradient of 11.5 mK/m (Kukkonen, 1993). Present temperature increase in the first 800 m is only about 9 °C. Heat flow and gradient values have been affected by the Pleistocene glaciations, but the low values are also indicative of an increased hydraulic conductivity and susceptibility for hydrothermal effects during the geological evolution. The Kivetty site was extensively studied in the 1990 s as a candidate site for nuclear waste disposal, and several hydrothermally altered, porous and permeable structures and hydrothermal bentonite as fracture filling were reported (Anttila et al., 1999; Saksa et al., 1998; Gehör et al., 1998; Reijonen et al., 2024). One of these structures is located beneath the bottom of the KiKR-1 borehole sampled for AFT analyzes (Green et al., 2022). The age of the alteration is not known, but we postulate that it may be Devonian, with a possible hydrothermal effect on AFT ages.

At the Jõhvi site the thermal history of the uppermost sample does not pop up among the others (Fig. 3), however, a deviation is present from the expected vertical age trend in the whole data set (Fig. 7). A decreasing AFT age trend with depth is not present, instead there is a weak increasing trend. Present temperatures of the Jõhvi samples are 14.5–21.3 °C. The samples are close to the SCPP surface with the uppermost sample only a few meters below the unconformity. Hydrothermal effects are possible here too; however, relevant geological evidence is not available. Nevertheless, hydrothermal Pb-Zn mineralization cross-cutting the crystalline basement and spreading into overlying Ediacaran sandstones has been reported from the Sonda-Uljaste-Haljala area (Sundblad et al., 1999) about 25 km to the west of Jõhvi site.

The sample from Attu (Fig. 1, Table 1) is from a drill hole penetrating the Paleoproterozoic Attu Zn-Cu-Pb massive sulphide deposit. The deposit is strata bound and interpreted to have a submarine exhalative origin (Hangala, 1987). Hydrothermal alteration is common in the host rocks of the deposit, suggesting that such activity occurred in the Precambrian. The deposit has not been studied for later mobilization of metals, but one of the known hydrothermal Devonian galena-sphalerite veins known in Finland (Alm and Sundblad, 2002; Alm et al., 2005; see section 5.5), in Västanfjärd, SW Finland, is located at less than 20 km from Attu.

5.5. Silurian-Devonian hydrothermal activity and AFT data

Paleozoic hydrothermal alteration is extensive in Fennoscandia comprising vein mineralization and Pb mobilization in the shield and dolomitization of limestones in the Baltic paleobasin (Pichugin et al., 1977; Tullborg et al., 1995; Larson and Tullborg, 1998; Alm et al., 2005; Alm and Sundblad, 2002). Low-temperature fluorite-calcite-galena-sphalerite-REE mineralization occurs in the shield and along its margins as fracture fillings and narrow veins in the Precambrian crystalline basement or as pore fillings in Ediacaran to Lower Cambrian sandstones.

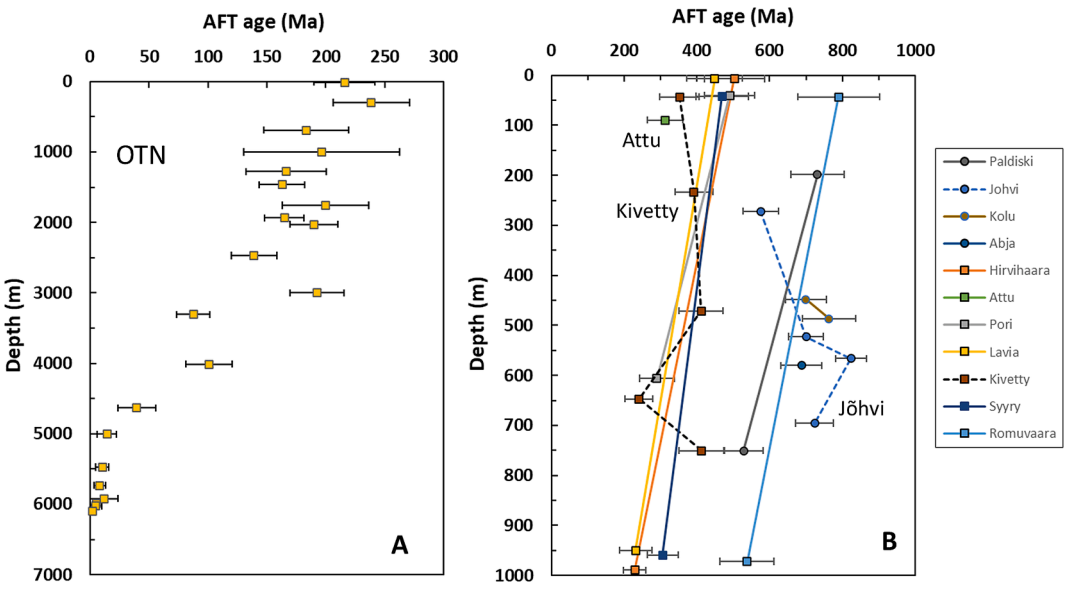


Fig. 7. Vertical variation of central ages with 2 sigma error bars a) in the superdeep OTN boreholes in southern Finland, b) in shallow (< 1 km deep) boreholes in Finland and Estonia. Only one sample was analyzed in Attu and Abja. The data sets interpreted to have hydrothermal effects are highlighted (Attu, Kivetty and Jõhvi). For location of boreholes, see Fig. 1 and Table 1. Data for OTN, Hirvihaara, Attu, Pori, Lavia, Kivetty, Syyry and Romuvaara sites are from Green et al. (2022). (For interpretation of the references to colour in this figure legend, the reader is referred to the web version of this article.)

Some of these are of economic interest (e.g., the Laisvall and Vassbo Pb deposits along the Caledonian front in Sweden) indicating significant mobilization of metals. The genesis and age of the mineralization have been frequently discussed in the literature (Billström et al., 2020). We propose that the vein-filling genesis is linked to the Caledonian orogeny and hydrothermal effects suggested by the AFT data, as well as the dolomitization of Ordovician and Silurian limestones in Estonia (Pichugin et al., 1977).

Alm et al. (2005) dated the veins in the shield with the Sm-Nd method on co-existing calcite-fluorite pairs to be 410–415 Ma. Thus, a hydrothermal system has operated on the scale of Fennoscandia in the Early Devonian. In previous studies it has been difficult to explain extensive fluid activity in the absence of any coeval magmatic activity in the shield. Alm et al. (2005) related the hydrothermal activity with the southeastwards migrating Caledonian thrust front in the Late Silurian to Early Devonian. According to Tullborg et al. (1995), stable oxygen isotope data on Ordovician limestones in Sweden together with conodont alteration, illite crystallinity, organic material maturation, apatite fission track and Pb mobilization data indicate increased paleotemperatures due to a mainly Devonian sedimentary cover deposited on the Cambrian-Silurian sequence. Further, Larson and Tullborg (1998), interpreted regional Pb mobilization and Paleozoic lower intercepts on the zircon U-Pb concordia as suggesting hydrothermal alteration under a ~ 2–4 km thick sedimentary cover. We attribute the hydrothermal activity to the Caledonian orogeny ranging from Late Silurian to Early Devonian with collision and thrusting peaking at 425 ± 25 Ma (Dunlap and Fossen, 1998). Pore pressure of the wet sediments experienced a dramatic increase due to burial beneath the thrust sheets, and pore fluids were expelled towards the craton along permeable cover sediments. Fluids gained heat from burial and were mineralized by dissolving elements from crustal rocks and the cover sediments and transported metals which finally precipitated in the fluorite-calcite-galena-sphalerite veins. Fluids could also have been partly meteoric and been recharged in the mountains of the thrust belt. Porous sandstones, thrust faults and well-developed horizontal fracture systems in granites provided excellent pathways for the hydrothermal fluids. Pb-Zn deposits would be expected to have been formed in the permeable sediments beneath the thrust sheets, the foredeep and the forebulge area. A similar hydrothermal origin has been suggested for the North American Mississippi Valley (MVT) type Pb-Zn deposits (Oliver, 1986; Fyfe and Kerrich, 1985).

The illite–smectite transition of Lower Cambrian clay in Estonia has been interpreted as either diagenetic or hydrothermal. Chaudhuri et al. (1999) determined the K-Ar age of illite in Cambrian clay as 380 Ma and attributed it to a hydrothermal origin. Środoń et al. (2009) reported K-Ar ages of Ordovician and Silurian K-bentonites (Bergström et al., 1995) in Norway, Sweden, Denmark, Poland and Estonia, and found support for both diagenetic and hydrothermal origins for illite. Similarly, Somelar et al., 2009, and Somelar et al., 2010 suggested that the illitization of Paleozoic clay-rich sediments in the Baltic paleobasin was controlled by the combination of burial diagenesis and influx of K-rich fluids. According to Kirsimäe et al. (2020) the illite of Cambrian clays was produced by diagenesis under normal geothermal conditions, but over a long period. The illite–smectite transition indicates a maximum paleotemperature of 50 °C. The question of illite origin remains equivocal.

Ordovician and Silurian limestones in southern and southeastern Estonia show massive dolomitization with a tectonic control (Pichugin et al., 1977). Dolomitization was due to hydrothermal activity along subvertical SW-NE and SE-NW faults. These faults were initiated in the Baltic basin by a NW-SE compression in Silurian – Devonian time (Šliaupa and Hoth, 2011; Tuuling, 2019). Dolomitization is not observed in Devonian sediments, and stratigraphic evidence implies it occurred before Mid-Devonian (>~395 Ma) (Pichugin et al., 1977). Polymetallic mineralization of MVT type (Davies and Smith, 2006) is associated with cavernous dolomites in Lower Silurian limestones, which carry Pb, Zn and Fe sulfides in brecciated rock (Pichugin et al., 1977; Vaher et al., 1961) and vein deposits in altered dolomitized rock (Eensaar et al., 2017).

The Estonian dolomites and their MVT deposits are analogous to hydrothermal dolomites occurring globally (Davies and Smith, 2006; Paradis et al., 2007). Hydrothermal dolomite formations have been studied intensively as they are important reservoir rocks in hydrocarbon geology due to the significant increase of their porosity by the replacement of Ca by Mg in the carbonate mineral lattice (Schön, 2004). Oliver (1986) linked the MVT deposits and the maturation and migration of hydrocarbon deposits in North America to Appalachian fluid expulsion. Interestingly, asphaltite (bitumen) occurrences have been reported in the Svecofennian basement in southern central Sweden as fracture

fillings and in breccias at depths < 150 m, i.e., in the vicinity of the SCPP surface. According to carbon isotope data, the asphaltite in Forsmark, central Sweden, is of biogenic origin with the Cambrian alum shale as a likely potential source rock (Sandström et al., 2006; Drake et al., 2017).

Paleomagnetic data have revealed hydrothermal components in rock remanences. Faults and shear zones in southern Finland carry secondary remanent magnetizations indicating hydrothermal influence of warm (<150 °C) oxidizing fluids (Mertanen et al., 2008). Plotting the poles on the apparent polar wander (APW) path of northern Europe (Torsvik et al., 1996) allows estimation of the age of the remanences. The ages obtained are Permian (250–300 Ma) and Silurian-Devonian (ca. 440 Ma and 415 Ma) (Mertanen et al., 2008; Preeden et al., 2009). Permian secondary remanences have also been reported from Ordovician dolomitized limestones in Estonia (Plado et al., 2010). As dolomitization is accompanied by the recrystallization of magnetic minerals (magnetite and hematite) (e.g., Elmore et al., 1985; Elmore et al., 1998), Mertanen et al. (2008) suggest that the dolomitization of Estonian limestones was coeval with the shearing-related secondary remanent magnetization. Thus, dolomitization most probably took place in Silurian-Devonian time at 440–415 Ma, i.e., during Caledonian thrusting, and again later in the Permian during the late stages of Pangea amalgamation when the thinning of sedimentary cover allowed meteoric fluids to penetrate to Ordovician strata.

The available evidence for craton-wide calcite-fluorite-Pb-Zn veins, MVT deposits, dolomitic alteration of Ordovician-Silurian limestones, and the debated origin of illite of the Lower Cambrian clay can be wrapped into a model of expulsion of hydrothermal fluids by the Caledonian orogeny. The main pathway for the fluids was provided by the Cambrian sediments, especially sandstone, which even today is porous, hardly consolidated and has high hydraulic permeability (Tšeban, 1975; Jõeleht and Kukkonen, 1996; Perens and Vallner, 1997). Further, the main decollement of the Caledonian thrusting was in the Cambrian alum shales, and the present extent of these thrusting surfaces has been mapped using seismic methods (Juhojuntti et al., 2001; Gee et al., 2010; Juhlin et al., 2019; Gee, 2021). Alum shales are rich in metals (U, Mo, V, Ni, Zn, Cd and Pb), REE and organic matter and provide a potential source for the mobilized elements (Leventhal, 1991) and bitumen (Dahl et al., 1989). Additionally, hydrocarbon generation from organic matter in the alum shale possibly increased pore pressures which assisted the thrusting (Morley, 1992). Fluid flow through the Cambrian sediments distributed warm fluids across Fennoscandia, impacting the crystalline bedrock below and the overlying Ordovician-Silurian sediments through fractures and faults.

Homogenization temperatures of fluid inclusions (15–25 eq. wt% $CaCl_2$-NaCl) in the calcite-fluorite-Pb-Zn veins in the shield are 80–150 °C (Alm and Sundblad, 2002; Alm et al., 2005) with a weak trend of decreasing temperatures to the southeast. Such hot fluid flow over tens of Ma could disturb the AFT annealing system and the mineral geochemistry (Green and Duddy, 1986; Steckler et al., 1993; Duddy et al., 1994, 1998; Filip et al., 2007, Kohn et al., 2024). We modelled the fluid expulsion with a fracture flow model by Bodvarsson (1969). Fluid expelled at 150 °C from the thrust belt would still be about 80–100 °C up to a distance of 400 km (Fig. 8). The composition of the fluids in the fluid inclusions in the shield are Ca-Na-Cl brines (Alm and Sundblad, 2005). Mg required for replacing Ca in limestone was conceivably derived from saline pore fluids in the sediments and the crystalline basement, analogous to present Cl-Na-K-Ca-Mg compositions of crustal saline fluids (Frape and Fritz, 1987; Nurmi et al., 1988; Bucher and Stober, 2010). The fluid pressure from the thrust front mobilized the fluids *in situ* in the Cambrian sediments and partly in the crystalline basement. This resulted in low temperature dolomitization of limestone followed by the later arrival of hydrothermal Pb and Zn and REE carrying fluids.

5.6. Implications for the present topography in Norway

There is a long debate over the origin of the present-day topography in Norway (e.g. Riis, 1996; Lidmar-Bergström et al., 2000; Nielsen et al., 2009a, b; Lidmar-Bergström and Bonow, 2009; Green et al., 2022; Hestnes et al., 2024). Rocks exhumed in the Caledonian Scandes mountains are Precambrian and Paleozoic, and expected to have eroded away a long time ago (Harrison, 1994; Reiners and Brandon, 2006; Tucker 2015), but nevertheless the topography is high, up to 2.5 km. Much of the controversy of the debate is related to the interpretation of low-relief planar surfaces located at considerable altitude, and whether the exhumation took place as one long process since the end of the Caledonian (Nielsen et al., 2009a) or whether there were several cyclic periods of uplift and subsidence (Lidmar-Bergström and Bonow, 2009; Nielsen et al 2009b). Geomorphological interpretations typically explain the planar surfaces at high elevations as paleic surfaces in the Davisian sense (Davis, 1899), i.e., as remains of genuine peneplains uplifted from sea level to present elevation by tectonic movements (e.g. Peulvast, 1985; Doré, 1992; Riis, 1996, Lidmar-Bergström et al., 2000), while explanations based on thermochronological data and isostasy do not necessarily accept them as peneplains (Nielsen et al., 2009a; Hestnes et al., 2024). The Davisian interpretation of the planar surfaces as ancient peneplains is challenged as no contemporary peneplains seem to exist (Phillips, 2002). Instead, the relief of mountain ranges develops as a dynamic system reflecting elevation and slope dependent erosion, isostatic response of the lithosphere, erosional unloading, or depositional loading as well as eustatic sea-level variations, climatic factors, and vegetation cover (Tucker, 2015).

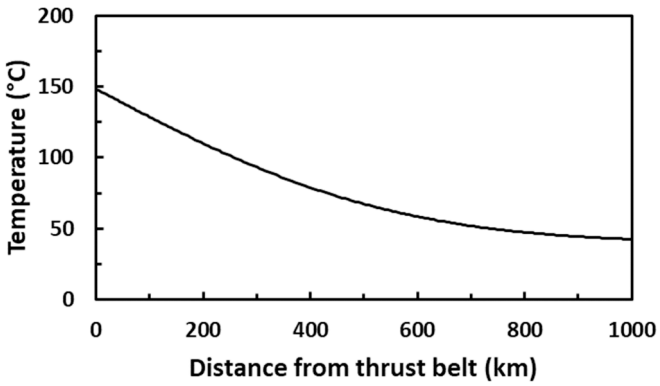


Fig. 8. Model for the temperature of the fluid expelled from the Caledonian thrust belt. An analytical solution of flow and heat transfer in a horizontal fracture was applied (Bodvarsson, 1969). Vertically recharging fluid enters a horizontal 100 m thick permeable layer at x = 0 (the thrust front) with an initial temperature of 150 °C and thereafter flows horizontally to the right in a formation with an initial temperature of 40°C. Permeability 10^{-13} m^2, porosity 20 %, hydraulic gradient 0.01, rock thermal conductivity 2 $Wm^{-1}K^{-1}$, and duration of flow 50 Ma.

In the ICE ('Ice-Climate-Erosion') model of Nielsen et al. (2009a) the present topography in southern Norway is viewed as the result of Caledonian collapse-driven exhumation later modified by enhanced glacial erosion since the climatic deterioration at the Eocene–Oligocene boundary. Modelers accepting the planar surfaces as genuine peneplains once eroded to sea-level suggest several periods of uplift and subsidence ranging from Late-Jurassic to Miocene (Lidmar-Bergström et al., 2000; Fjellanger and Etzelmüller, 2003; Lidmar-Bergström and Bonow, 2009; Japsen et al., 2018; Japsen and Chalmers, 2022; Green et al., 2022). Theoretically, such developments should be represented in LTT data, but overprinting by younger burial periods, the resolution of the methods and ambiguities of inverse modeling do not allow for a straightforward interpretation. Cyclic uplift-subsidence periods with a decreasing trend of burial temperatures from one cycle to the next may be fitted within the uncertainties of the LTT data as well as by a monotonous cooling trend (e.g., Kohn et al., 2024).

In a recent contribution to the debate, Hestnes et al. (2024) tested different models with AFT and apatite (U-Th)/He data from two

elevation sample transects in southern Norway (see section 5.3). The best fit of modelled t-T histories (Hestnes et al., 2024) was obtained with a simple model suggesting rapid cooling after orogenic collapse up to the late Permian followed by slower cooling during Triassic – Cretaceous and accelerated cooling again in the Cenozoic (see also 5.3). This thermal history scenario is in agreement with the cooling t-T histories inverted here from the Finnish and Estonian AFT data (Fig. 5). Cooling in the Jurassic to surface conditions, as suggested by Lidmar-Bergström et al. (2000), is theoretically within the acceptance limits of the inverse models but would require rapid burial to 1.5–3 km and re-exhumation in the Cenozoic. A Miocene uplift, also included in the planar surface interpretations (Lidmar-Bergström et al., 2000), cannot be excluded. However, this is primarily due to the LTT methods applied not being sensitive to the low temperature ranges involved.

In the framework of our model, the AFT data analyzed in the present paper, the results of Hestnes et al. (2024) as well as the late-orogenic and pre-drift developments of southern and mid Norway and the continental margin (Dunlap and Fossen, 1998; Fossen and Dunlap, 1998; Torsvik et al., 2001; Walsh et al., 2013; Færseth, 2021) all agree with an interpretation of the topography and relief evolving from orogenic collapse and exhumation in the Devonian. A rejuvenation of the topography began almost seamlessly following orogenic collapse at the Devonian – Carboniferous boundary by pre-drift extension and uplift in the Carboniferous – Cretaceous (Fig. 5). The uplift was accelerated in the Cenozoic after continental break-up and separation of the plates.

Exhumation during orogenic collapse and thereafter was a process driven by both tectonics and isostasy. Thinning of the lithospheric mantle produced buoyancy (section 5.3) driving the rejuvenation of topography from the Carboniferous. Isostatic compensation allows topography to evolve in a dynamic balance between erosion and buoyancy, thus preserving mountainous relief according to Hack's (1960) theory of erosional topography. In Hack's model, the relief and scenery achieve a steady-state condition, though the crust is continuously exhumed bringing rocks from depth to surface level (Braun et al., 2006).

As indicated previously the t-T histories inverted by Hestnes et al. (2024) for southern Norway imply that from Permian to present erosion rates were variable and marked by low rates (ca. 6 m/Ma) between 250–75 Ma. The low Mesozoic erosion rates may indicate there was an elevated plateau with little relief, analogous to the present Tibetan plateau regardless of high altitude (Ouimet et al., 2009; Tucker, 2015). This would agree with the findings of Dunlap and Fossen (1998) indicating there was still ca. 1.5 km high topography in southern Norway between orogenic collapse at ca. 400 Ma and the late Permian. K-Ar and $^{40}Ar/^{39}Ar$ data suggest that the exhumation of the high-grade gneiss region progressed westward at 400–380 Ma exhuming mid-crustal rocks earlier in the east than in the west. The exhumation pattern was caused primarily by E–W stretching, but also by eastward tilting and differential exhumation, depending on the area (Walsh et al. 2013). Together with brittle–ductile and brittle fault data the results indicate that exhumation along local structures continued into the Permian (Eide et al. 1997; Hacker et al., 2010; Walsh et al., 2013).

In the Caledonian orogen in the southern Appalachian Great Smoky Mountains, which was never glaciated, erosion rates during orogenic processes were high (>100 m/Ma), followed by much slower rates over the next 180 Ma up to present (25–30 m/Ma). Under a humid climate the Smoky Mountains, with highest peaks ca. 1,500 m above sea level, are covered by vegetation. Isostasy-driven erosion has reached a dynamic equilibrium, and mass is removed at the same rate in all parts of drainage basins of the Smoky Mountains on times scales of 10^4–10^5 years (Matmon et al., 2003). In the case of the Smoky Mountains, Hack's theory (Hack, 1960) seems to be correct. We consider the Appalachian erosional development analogous to the southern Norwegian case during the Carboniferous – Jurassic. The Carboniferous was characterized by the global expansion of plant species, and the vegetation conceivably contributed positively to the preservation of the Caledonian topography (ca. < 1.5 km, Dunlap and Fossen, 1998) following orogenic collapse.

The origin of the paleic surfaces (Lidmar-Bergström et al., 2000, Fjellanger and Etzelmüller, 2003) remains enigmatic. Due to the lack of compelling evidence from sedimentary cover on their surfaces, their ages are not easy to constrain. Saprolites, such as kaolinite, suggest long-term deep weathering in the Mesozoic and Cenozoic (Lidmar-Bergström, 1995; Gilg et al., 2013). Lithological differences and geological structures were noted to be important for the interpretation of the paleic surface reliefs (Fjellanger and Etzelmüller, 2003). Paleomagnetic and structural evidence suggests that extensional deformational events were active in central southern Norway in the Permo – Triassic and Jurassic and extended up to the early Cretaceous. These ages correlate with major stages of rifting in north-central Pangaea and can be correlated directly with the main rift events in the North Sea (Andersen et al., 1999). We suggest that extensional flattening of the elevated topography during and after Caledonian collapse may have played an important role in creating the landscape and forming the planar surfaces shaped later by erosional and glacial processes especially in the Mezosoic – Cenozoic. Thus, the paleic surfaces may represent subhorizontal extension faults exhumed by erosion. Our present model is generally in line with that of Nielsen et al. (2009a), however, we suggest an active role of pre-drift extensional uplift activated in the Carboniferous and possibly accelerated in the Cenozoic.

5.7. Implications for deep biosphere

Our model of fluid expulsion during the Caledonian orogeny has important implications for the distribution and transport of microbial life forms in the subsurface. The continental and oceanic crust hosts extensive microbial life of archaea, bacteria, fungi, and viruses (Whitman et al., 1998; Onstott et al., 1999; Pedersen, 2000; Takai et al., 2001; Lin et al., 2005; Horsfield et al., 2007; Chivian et al., 2008; Kyle et al., 2008; Sahl et al., 2008; Nuppunen-Puputti et al., 2021). It is estimated that about 10–20 % of the entire prokaryote biomass of the earth lives beneath the surface (McMahon and Parnell, 2014; Magnabosco et al., 2018). The ecological niches are provided by pore and fracture spaces filled with saline fluids (Itävaara et al., 2011). At depths greater than about 100 m microbes are anaerobic, and do not receive energy from photosynthesis, instead, the organisms are chemolithoautotrophic, receiving their energy from appropriate chemical reactions (Gold, 1992; Pedersen, 1997, 2000).

The temperature limit for biological life is 121 °C (Kashefi & Lovley, 2003), which corresponds to a depth of about 4–6 km in the continental crust. Thus, a considerable portion of the upper crust in continents is habitable for life. Exposure to temperatures above 121 °C by burial, fluids or magmatic heating will sterilize the rock. However, after exhumation and cooling other microbes will migrate back to the depths which have become habitable again (Drake and Reiners, 2021; Drake et al, 2024). The hot fluids expelled along the thrust faults and the Cambrian sandstone in Fennoscandia will have first sterilized the microbial life forms encountered by the flow, but the expulsion set *in situ* fluids in motion ahead of the hot fluid front. This way, the existing microbial life forms were potentially transported hundreds of kilometers to the southeast within Fennoscandia and the East European platform. The mobilization and transport of elements and hydrocarbons (Leventhal, 1991; Dahl et al., 1989) in the hydrothermal fluid enlarged and rejuvenated the nutrient and energy resources in the Cambrian strata and affected the fracture networks in the underlying crystalline rock and overlying sedimentary rocks.

Fluid expulsions occur in every collisional orogeny in some form, and over the geological history of the Earth there have been hundreds of plate collisions. Therefore, collisional fluid expulsion may have positively affected the evolution, diversity, and preservation of subsurface life forms throughout earth history ever since plate tectonics became operational in the Eo – Paleoarchean (Kranendonk, 2011; Komiya et al., 2015; Cawood et al., 2018; Windley et al., 2021).

6. Conclusions

Apatite fission track data and inversions suggest consistent t-T histories for samples from Estonia and Finland. The Phanerozoic evolution of the Fennoscandian shield and the Paleo-Baltic basin is tightly connected to the Silurian – Devonian Caledonian orogeny and formation of the foredeep basin and forebulge uplift. In southern and central Finland, the Precambrian basement was exposed in the Phanerozoic for the first time during the Devonian forebulge but soon thereafter it was covered by sediments again to be finally exposed in the Mezozoic – Cenozoic. The orogenic collapse of the Caledonides, and the subsequent erosion and relaxation of the lithospheric flexure resulted in the covering of southern and central Finland with a thin sedimentary cover reaching its maximum thickness at the Carboniferous – Permian boundary.

The Paleo-Baltic basin was within the forebulge area of the Caledonides, but as it had previously been a basin since Cambrian times, it experienced only a mild inversion during the lithospheric relaxation. In the basin, sedimentary cover was at its thickest in the late Carboniferous. AFT paleotemperatures and illite–smectite transition temperatures of Cambrian clay suggest that sediments were up to ca. 0.5 km thicker in Estonia than today and up to ca. 1.5 km thick in Finland.

The development towards the opening of the North Atlantic began with lithospheric extension and gradual uplift of the exhumed Caledonian belt and surrounding areas from early Permian to mid-Jurassic. The uplift is recorded by reconstructed AFT paleotemperatures in Estonia and Finland which start to decrease from ca. 300 Ma. The uplift was due to thinning of the Caledonian lithospheric mantle which was still warm and rheologically weak after orogenic crustal thickening. The whole of Fennoscandia experienced uplift and tilting of the lithosphere towards the southeast from the late Carboniferous. When the North Atlantic finally opened at ca. 54 Ma, the Baltic and Greenland plates separated resulting in an increase in buoyancy of the margin and acceleration of uplift in the Paleogene.

The SCPP surface, forming an important geological constraint for thermal history modeling, originally formed by denudation of Baltica in the Neoproterozoic experienced deformation into a domal shape by the Caledonian elastic flexure of the lithosphere. In the Mesozoic – Cenozoic the SCPP surface was gradually eroded in Finland revealing the present MCHT surface.

The AFT results also indicate hydrothermal effects. We attribute these to the expulsion of hot fluids from the Caledonian thrust belt to the basal Cambrian sediments and the crystalline basement. Evidence for Devonian hydrothermal activity is known craton-wide as the Devonian age calcite-fluorite-Pb-Zn veins, Mississippi Valley type Pb-Zn deposits in the Caledonian front, dolomitic alteration of Ordovician-Silurian limestones in Estonia as well as secondary Devonian magnetizations in shear zones of the basement in Finland. The fluid expulsion further implies that microbial life forms present in the pore and fracture fluids were transported by hundreds of km to the southeast in Fennoscandia and surroundings. Therefore, as continent–continent collisions have not been infrequent in geological history, collisional fluid expulsion may have affected the evolution, diversity, and preservation of subsurface life forms throughout earth history.

Our model contributes to the interpretation of the evolution of topography in Norway. After the orogenic collapse of the Caledonian mountain range in the Devonian there was still considerable topography in southern Norway and a large emergent land mass in the area of the present Norwegian Sea up to late Jurassic time. Pre-drift extension and uplift began to rejuvenate the topography from the early Permian, a process accelerated in the Paleogene after continental break-up. Thus, the present topography was partly inherited from the original mountain belt, but with a contribution by Carboniferous – Jurassic pre-drift extension and uplift. We provide a new alternative interpretation for the debated planar surfaces at high altitude in southern Norway which have traditionally been interpreted as uplifted ancient peneplains. These surfaces may actually be extensional structures formed during extensional collapse and flattening of the Caledonides and shaped later by erosional and glacial processes.

CRediT authorship contribution statement

Ilmo T. Kukkonen: Writing – review & editing, Writing – original draft, Visualization, Methodology, Investigation, Conceptualization. **Barry Kohn:** Writing – review & editing, Methodology, Investigation, Conceptualization. **Kalle Kirsimäe:** Writing – review & editing, Investigation, Conceptualization. **Argo Jõeleht:** Writing – review & editing, Investigation, Conceptualization. **Ling Chung:** Writing – review & editing, Investigation. **Malcolm McMillan:** Writing – review & editing, Investigation. **Samuel Boone:** Writing – review & editing, Data curation. **Andy Gleadow:** Writing – review & editing, Methodology, Conceptualization.

Declaration of Competing Interest

The authors declare that they have no known competing financial interests or personal relationships that could have appeared to influence the work reported in this paper.

Acknowledgments

The present research was carried out during the first author's sabbatical visit to the University of Melbourne in 2024. The University of Melbourne thermochronology laboratory has received substantial infrastructure funding under Projects 3.51, 3.1252 and the AGOS Geohistory Project through the AuScope program (www.auscope.org.au) of the Australian National Collaborative Research Infrastructure Strategy (NCRIS). Significant equipment support has also been received through the Australian Research Council LIEF program (LE0882818, LE0989067). The manuscript was reviewed by Chris Morley, Jan Martin Huizenga and an anonymous reviewer.

Appendix A. Supplementary data

Supplementary data to this article can be found online at https://doi.org/10.1016/j.gr.2025.05.011.

References

Abbey, A.L., Wildman, M., Stevens Goddard, A.L., Murray, K.E., 2023. Thermal history modeling techniques and interpretation strategies: Applications using QTQt. Geosphere 19, 493–530, Doi: 10.1130 /GES02528.1.

Abels, A., Plado, J., Pesonen, L.J., Lehtinen, M., 2002. The Impact Cratering Record of Fennoscandia — a Close look at the Database. In: Plado, J., Pesonen, L.J. (Eds.), Impacts in Precambrian Shields. Impact Studies. Springer, Berlin, Heidelberg. https://doi.org/10.1007/978-3-662-05010-1_1.

Aldridge, R.J., 1984. Thermal metamorphism of the Silurian strata of the Oslo region, assessed by conodont colour. Geol. Mag. 121, 347–349.

Alm, E., Sundblad, K., 2002. Fluorite-calcite-galena-bearing fractures in the counties of Kalmar and Blekinge, Sweden. Swedish Nuclear Fuel and Waste Management Co, SKB Report R-02-42, p. 116.

Alm, E., Sundblad, K. Huhma, H., 2005. Sm-Nd isotope determinations of low-temperature fluorite-calcite-galena mineralization in the margins of the Fennoscandian Shield — Report of activities carried out during 2004. Swedish Nuclear Fuel and Waste Management Co, SKB Report R-05-66, p. 58.

Andersen, T., Taylor, P.N., 1988. Pb isotope geochemistry of the Fen carbonatite complex, S.E. Norway: Age and petrogenetic implications. Geomchim. Cosmochim. Acta 52, 209–215.

Andersen, T.B., Jamtveit, B., Dewey, J.F., Swensson, E., 1991. Subduction and eduction of continental crust: major mechanism during continent–continent collision and orogenic extensional collapse, a model based on the south Norwegian Caledonides. Terra Nova 3, 303–310.

Andersen, T.B., Torsvik, T.H., Eide, E.A., Osmundsen, P.T., Faleide, J.I., 1999. Permian and Mesozoic extensional faulting within the Caledonides of central south Norway. J. Geol. Soc. 156, 1073–1080.

Anell, I., Thybo, H., Artemieva, I.M., 2009. Cenozoic uplift and subsidence in the North Atlantic region: Geological evidence revisited. Tectonophysics 474, 78–105.

Anell, I., Thybo, H., Stratford, W., 2010. Relating Cenozoic North Sea sediments to topography in southern Norway: the interplay between tectonics and climate. Earth Planet. Sci. Lett. 300, 19–32.

Anttila, P., Ahokas, H., Front, K., Heikkinen, E., Hinkkanen, H., Johansson, E., Paulamäki, S., Riekkola, R., Saari, J., Saksa, P., Snellman, M. Wikström, L., Öhberg, A., 1999. Final disposal of spent nuclear fuel in Finnish bedrock – Kivetty site report. Report POSIVA 99-09, Posiva Oy, Helsinki, p. 206.
Axberg, S., 1980. Seismic stratigraphy and bedrock geology of the Bothnian Sea, northern Baltic. GFF 36, 153 - 213.
Bauert, H., 1993. The Baltic Oil Shale Basin: An Overview. In: Proceedings, 1993 Eastern Oil Shale Symposium, Nov. 16-19, Institute for Mining & Minerals Research, University of Kentucky, pp. 411–421.
Bergman, L., 1982. Clastic dykes in the Åland Islands, SW Finland and their origin. Bull. Geol. Surv. Finland 317, 7–33.
Bergström, S.M., Huff, W.D., Kolata, D.K., Bauert, H., 1995. Nomenclature, stratigraphy, chemical fingerprinting, and areal distribution of some Middle Ordovician K-bentonites in Baltoscandia. GFF 117, 1–13. https://doi.org/10.1080/11035899509546191.
Berthelsen, A., 1980. Towards a palinspastic tectonic analysis of the Baltic Shield. In: Cogne, J., Slansky, M. (Eds.), Geology of Europe, from Precambrian to the Post-Hercynian Sedimentary Basins. Memoires du B.R.G.M, pp. 5–21.
Berthelsen, A., 1992. From Precambrian to Variscan Europe. In: Blundell, D., Freeman, R., Mueller, S.t. (Eds.), A Continent Revealed: the European Geotraverse. Cambridge University Press, Cambridge, pp. 153–164.
Billström, K., Broman, C., Larsson, A., Schérsten, A., Schmitt, M., 2020. Sandstone-hosted Pb-Zn deposits along the margin of the Scandinavian Caledonides and their possible relationship with nearby Pb-Zn vein mineralization. Ore Geol. Rev. 127, 103839. https://doi.org/10.1016/j.oregeorev.2020.103839.
Bingen, B., Nordgulen, Ø., Viola, G., 2008. A four-phase model for the Sveconorwegian orogeny, SW Scandinavia. Norwegian J. Geol. 88, 43–72.
Bodvarsson, G., 1969. On the temperature of water flowing through fractures. J. Geophys. Res. 74, 1987–1992.
Bogdanova, S., Gorbatschev, R., Grad, M., Janik, T., Guterch, A., Kozlovskaya, E., Motuza, G., Skridlaite, G., Starostenko, V., Taran, L., Eurobridge, Polonaise Working Groups, 2006. EUROBRIDGE: new insight into the geodynamic evolution of The East European Craton. In: Gee, D.G., Stephenson, R.A. (Eds.), European Lithosphere Dynamics, vol. 32. Geol. Soc., London, Memoirs, pp. 599–625.
Boone, S.C., Dalton, H., Prent, A., Kohlmann, F., Theile, M., Gréau, Y., Florin, G., Noble, W., Hodgekiss, S.A., Ware, B., Phillips, D., Kohn, B., O'Reilly, S., Gleadow, A., McInnes, B., Rawling, T., 2022. AusGeochem: an open platform for geochemical data preservation, dissemination and synthesis. Geostand. Geoanal. Res. 46 (2), 245–259.
Boone, S.C., Kohlmann, F., Noble, W., Theile, M., Beucher, R., Kohn, B., Glorie, S., Danišík, M., Zhou, R., McMillan, M., Nixon, A., 2023. A geospatial platform for the tectonic interpretation of low-temperature thermochronology big Data. Sci. Rep. 13 (1), 8581.
Braun, J., van der Beek, P., Batt, G., 2006. Quantitative thermochronology – Numerical methods for the interpretation of thermochronological data. Cambridge Univ Press, p. 258.
Buchardt, B., Nielsen, A.T., 1985. Carbon and oxygen isotope composition of Cambro-Silurian limestone and anthraconite from Bornholm: evidence for deep burial diagenesis. Bull. Geol. Soc. Denmark 33, 415–435.
Bucher, K., Stober, I., 2010. Fluids in the upper continental crust. Geofluids 10, 241–253.
Cawood, P.A., Hawkesworth, C.J., Pisarevsky, S.A., Dhuime, B., Capitanio, F.A., Nebel, O., 2018. Geological archive of the onset of plate tectonics. Philos. Trans. Roy. Soc. A 376, 20170405. https://doi.org/10.1098/rsta.2017.0405.
Cederbom, C., Larson, S.A., Tullborg, E.-L., Stiberg, J.-P., 2000. Fission track thermochronology applied to Phanerozoic thermotectonic events in central and southern Sweden. Tectonophysics 316, 153–167.
Chaudhuri, S., Srodon, J., Clauer, N., 1999. K-Ar dating of illitic fractions of Estonian "Blue Clay" treated with alkylammonium cations. Clays Clay Miner. 47, 96–102.
Chivian, D., Brodie, E.L., Alm, E.J., et al., 2008. Environmental genomics reveals a single-species ecosystem deep within Earth. Science 322, 275–278.
Cloetingh, S.A.P.L., 1988. Intraplate stresses: a new element in basin analysis. In: New perspectives in Basin Analysis, Springer Verlag, pp. 205–230.
Dahl, J., Chen, R.T., Kaplan, I.R., 1989. Alum Shale bitumen maturation and migration: Implications for Gotland's oil. J. Petroleum Geol. 12, 465–476.
Davies, G.R., Smith, L.B., 2006. Structurally controlled hydrothermal dolomite reservoir facies: an overview. AAPG Bull. 90, 1641–1690.
Davis, W.M., 1899. The geographical cycle. Geogr. J. 14, 481–504.
DeCelles, P.G., 2012. Foreland basin systems revisited: variations in response to tectonic settings. In: Busby, C., Azor Pérez, A., (Eds.), Tectonics of Sedimentary Basins: Recent Advances, First Edition, Blackwell Publishing, pp. 405–426.
Degeai, J.-P., Peulvast, J.-P., 2006. Calcul de l'érosion à long terme en région de socle autour de grands astroblèmes du Québec et de France. Géog. Phys. Quatern. 60, 131–148.
Donelick, R.A., Miller, D.S., 1991. Enhanced tint fission track densities in low spontaneous track density apatites using ^{252}Cf-derived fission fragment tracks: a model and experimental observations. Int. J. Radiat. Appl. Instrum. Part D 18, 301–307.
Donelick, R.A., O'Sullivan, P.B., Ketcham, R.A., 2005. Apatite fission-track analysis. Rev. Miner. Geochem. 58, 49–94.
Doré, A.G., 1992. The Base Tertiary Surface of southern Norway and the northern North Sea. Norw. J. Geol. 72, 259–265.
Doré, A.G., Cartwright, J. A., Stoker, M. S., Turner, J.P., White, N. J., 2002. Exhumation of the North Atlantic margin: introduction and background. In: A.G. Dore, J.A. Cartwright, M.S. Stoker, J.P. Turner and N.J. White, Exhumation of the North Atlantic Margin: Timing, Mechanisms and Implications for Petroleum Exploration. Geol. Soc. London, Spec. Publ. 196, 1–12.
Drake, H., Heim, C., Roberts, N.M.W., Zack, T., Tillberg, M., Broman, C., Ivarsson, M., Whitehouse, M.J., Åström, M.E., 2017. Isotopic evidence for microbial production and consumption of methane in the upper continental crust throughout the Phanerozoic eon. Earth Planet. Sci. Lett. 470, 108–118.
Drake, H., Makahnouk, W.R.M., Roberts, N.M.W., Reinhardt, M., Henkemans, E., Frape, S.K., Tullborg, E.-L., Broman, C., Whitehouse, M.J., Kooijman, E., 2024. Late cretaceous and Early Paleogene Fluid Circulation and Microbial activity in Deep Fracture Networks of the Precambrian Basement of Western Greenland. Geochem. Geophys. 25, e2024GC011646. https://doi.org/10.1029/2024GC011646.
Drake, H., Reiners, P.W., 2021. Thermochronologic perspectives on the deep-time evolution of the deep biosphere. PNAS 118 (45), e2109609118. https://doi.org/10.1073/pnas.2109609118.
Duddy, I.R., Green, P.F., Bray, J.R., Hegarty, K.A., 1994. Recognition of the thermal effects of fluid flow in sedimentary basins. In: Parnell, J. (ed.), Geofluids: Origin, Migration and Evolution of Fluids in Sedimentary Basins, Geol. Soc. Spec. Publ. 78, 325–345.
Duddy, I. R., Green, P. F., Hegarty, K. A., Bray, R. J., O'Brien, G.W. 1998. Dating and duration of hot fluid flow events determined using AFTA. In: Parnell, J. (ed.) 1998. Dating and Duration of Fluid Flow and Fluid-Rock Interaction. Geol. Soc. London, Spec. Publ. 144, 41–51.
Dunlap, W.J., Fossen, H., 1998. Early Paleozoic orogenic collapse, tectonic stability, and late Paleozoic continental rifting revealed through thermochronology of K-feldspars, southern Norway. Tectonics 17, 604–620.
Eensaar, J., Gaškov, M., Pani, T., Sepp, H., Somelar, P., Kirsimäe, K., 2017. Hydrothermal fracture mineralization in the stable cratonic northern part of the Baltic Paleobasin: sphalerite fluid inclusion evidence, GFF139, 52–62, Doi: 10.1080/11035897.2016.1196499.
Ehlers, T.A., Farley, K.A., 2003. Apatite (U-Th)/He thermochronometry: methods and applications to problems in tectonic and surface processes. Earth Plan. Sci. Lett. 206, 1–14.
Eide, E.A., Torsvik, T.H., Andersen, T.B., 1997. Absolute dating of brittle fault movements: late Permian and late Jurassic extensional fault breccias in western Norway. Terra Nova 9, 135–139.
Elming, S.-Å., Pesonen, L.J., Leino, M.A.H., Khramov, A.N., Mikhailova, N.P., Krasnova, A.F., Mertanen, S., Bylund, G., Terho, M., 1993. The drift of Fennoscandian and Ukrainian shields during the Precambrian: a palaeomagnetic analysis. Tectonophysics 223, 177–198.
Elmore, R.D., Dunn, W., Peck, C., 1985. Absolute dating of dedolomitization by means of paleomagnetic techniques. Geology 13, 558–561.
Elmore, R. D., Campbell, T., Banerjee, S., Bixler, W. G. 1998. Palaeomagnetic dating of ancient fluid-flow events in the Arbuckle Mountains, southern Oklahoma. In: Parnell, J. (ed.) Dating and duration of fluid flow and fluid-rock interaction. Geol. Soc. Spec. Publ. 144, pp. 9–25.
Enkelmann, E., Garver, J.I., 2016. Low-temperature thermochronology applied to ancient settings. J. Geodyn. 93, 17–30.
Esedo, R., van Wijk, J., Coblentz, D., Meyer, R., 2012. Uplift prior to continental breakup: Indication for removal of mantle lithosphere? Geosphere 8, 1078–1085. https://doi.org/10.1130/GES00748.1.
Fauconnier, J., Labrousse, J.L., Andersen, T.B., Beyssac, O., Duprat-Oualid, S., Yamato, P., 2014. Thermal structure of a major crustal shear zone, the basal thrust in the Scandinavian Caledonides. Earth Plan. Sci. Lett. 385, 162–171.
Færseth, R.B., 2021. The deep Møre and Vøring basins of the Norwegian Sea as basement highs prior to late Jurassic rifting. Norw. J. Geol. 101, 202113. https://doi.org/10.1785/njg101-3-3.
Filip, J., Ulrych, J., Adamovič, J., Balogh, K., 2007. Apatite fission track implications for timing of hydrothermal fluid flow in Tertiary volcanic of the Bohemian Massif. J. Geosci. 52 (2007), 211–220. https://doi.org/10.3190/jgeosci.014.
Fjellanger, J., Etzelmüller, B., 2003. Stepped palaeosurfaces in southern Norway - interpretation of DEM -derived topographic profiles. Norw. J. Geogr. 57, 102–110. https://doi.org/10.1080/00291950310001388.
Fleischer, R.L., Price, P.B., Walker, R.L., 1975. Nuclear tracks in solids: principles and applications. Univ. of California Press, Berkeley.
Floden, T.R., Jacobsson, M., Kumpas, G., Wadstein, P., Wannäs, K., 1979. Geophysical investigations of the western Bothnian Bay. GFF 101, 321–327.
Flowers, R.M., 2009. Exploiting radiation damage control on apatite (U–Th)/He dates in cratonic regions. Earth Plan. Sci. Lett. 277, 148–155.
Flowers, R.M., Bowring, S.A., Reiners, P.W., 2006. Low long-term erosion rates and extreme continental stability documented by ancient (U-Th)/He dates. Geology 34, 925–928. https://doi.org/10.1130/G22670A.1.
Fossen, H., Dunlap, W.J., 1998. Timing and kinematics of Caledonian thrusting and extensional collapse, southern Norway: evidence from 40Ar/39Ar thermochronology. J. Struct. Geol. 20, 765–781.
Frape, S. K., Fritz P., 1987. Geochemical trends for groundwaters from the Canadian Shield. In: P. Fritz and S. K. Frape (Eds), Saline Water and Gases in Crystalline Rocks, p. 19–38, Geol. Assoc. Canada Spec. Paper 33.
Friese, N., Vollbrecht, A., Leiss, B., Jacke, O., 2011. Cambrian sedimentary dykes in the Proterozoic basement of the Västervik area (southeast Sweden): episodic formation inferred from macro- and microfabrics. Int. J. Earth Sci. (geol Rundsch) 100, 741–752. https://doi.org/10.1007/s00531-009-0508-3.
Fyfe, W.S., Kerrich, R., 1985. Fluids and thrusting. In: Y. Kitano (Ed.), Water—Rock Interaction. Chem. Geol. 49, 353–362.
Gaál, G., Gorbatschev, R., 1987. An outline of the Precambrian evolution of the Baltic Shield. Precambr. Res. 35, 15–52.
Galbraith, R.F., 2005. Statistics for fission track analysis. Chapman & Hall/CRC, Boca Raton. doi:10.1198/jasa.2007.s165.

Gallagher, K., Ketcham, R.A., 2018. Comment on "Thermal history modelling: HeFTy vs. QTQt" by Vermeesch and Tian, Earth Sci. Rev. 139, 279–290". Earth Sci. Rev. 387–394.
Gee, D.G., 1975. A tectonic model for the central part of the Scandinavian Caledonides. Am. J. Sci. 275A, 468–515.
Gee, D., 2020. Swedish Caledonides: key components of an early–middle Paleozoic Himalaya-type collisional orogen. In: M.B. Stephens and & J. B Weihed (eds) 2020. Sweden: Lithotectonic Framework, Tectonic Evolution and Mineral Resources. Geol. Soc. Lond. Mem. 50, 577–599. Doi: 10.1144/M50-2019-20.
Gee, D., 2021. Caledonides of Scandinavia, Greenland and Svalbard. In: D. Alderton & S. A. Elias (eds), Encyclopedia of Geology, Elsevier, 2nd edition, Vol. 4, p. 311–326 Doi: 10.1016/B978-0-08-102908-4.00119-3 311.
Gee, D.G., Stephenson, R.A., 2006. The European lithosphere: an introduction. In: Gee, D.G. and Stephenson, R.A. (Eds.), European Lithosphere Dynamics. Geol. Soc. Lond. Mem. 32, 1 – 9.
Gee, D.G., Juhlin, C., Pascal, C., Robinson, P., 2010. Collisional Orogeny in the Scandinavian Caledonides (COSC). GFF 132 (1), 29–44. https://doi.org/10.1080/11035891003759188.
Gehör, S., Kärki, A., Taikina-aho, O., 1998. Kivetty, Äänekoski: Petrology and low temperature fracture minerals in the KI-KR12 and KI-KR13 drill cores. Working report 98-35, Posiva Oy, Helsinki, pp. 138.
Gibbard, P.L., Lewin, J., 2016. Filling the North Sea Basin: Cenozoic sediment sources and river styles. Geol. Belg. 19, 201–217. https://doi.org/10.20341/gb.2015.017.
Gilg, H.A., Hall, A.M., Ebert, K., Fallick, A.E., 2013. Cool kaolins in Finland. Palaeogeogr. Palaeoclimatol. Palaeoecol. 392, 454–462.
Gleadow, A.J.W., Duddy, I.R., 1981. A natural long-term track annealing experiment for apatite. Nucl. Tracks 5, 169–174.
Gleadow, A.J.W., Gleadow, S.J., Belton D.X., Kohn, B.P., Krochmal M.S., 2009. Coincidence Mapping a key strategy for automated counting in fission track dating. In: Ventura, B., Lisker, F., Glasmacher, U.A. (*eds.*), Thermochronological methods: from palaeotemperature constraints to landscape evolution models. Geol. Soc. London Spec. Publ. 324, 25–36.
Gold, T., 1992. The deep, hot biosphere. P. Natl. Acad. Sci. USA 89, 6045–6049.
Green, P.F., Duddy, I.R., 1986. Thermal annealing of fission tracks in apatite. Chem. Geol. (isotope Geoscience Section) 59, 237–253.
Green, P.F., Japsen, P., Bonow, J.M., Chalmers, J.A., Duddy, I.R., Kukkonen, I.T., 2022. The post-Caledonian thermo-tectonic evolution of Fennoscandia. Gondwana Res. 107, 201–234. https://doi.org/10.1016/j.gr.2022.03.007.
Guenthner, W.R., Reiners, P.W., Ketcham, R.A., Nasdala, L., Geister, G., 2013. Helium diffusion in natural zircon: radiation damage, anisotropy, and the interpretation of zircon (U-Th)/He thermochronology. Am. J. Sci. 313, 145–198. https://doi.org/10.2475/03.2013.01.
Hack, J.T., 1960. Interpretation of erosional topography in humid temperate regions. Am. J. Sci. 285, 80–97.
Hacker, B.R., Andersen, T.B., Johnston, S., Kylander-Clark, A.R.C., Peterman, E.M., Walsh, E.O., Young, D., 2010. High-temperature deformation during continental-margin subduction & exhumation: the ultrahigh-pressure Western Gneiss Region of Norway. Tectonophysics 480, 149–171.
Hall, A.M., Putkinen, N., Hietala, S., Lindsberg, E., Holma, M., 2021. Ultra-slow cratonic denudation in Finland since 1.5 Ga indicated by tiered unconformities and impact structures. Precambr. Res. 352, 106000. https://doi.org/10.1016/j.precamres.2020.106000.
Hall, A.M., Barfod, D.N., Gilg, H.A., Stuart, F.M., Sarala, P., Al-Ani, T., 2024. Intensive chemical weathering in the Arctic during the Miocene Climatic Optimum. Palaeogeogr. Palaeoclimatol. Palaeoecol. 634, 111927. https://doi.org/10.1016/j.palaeo.2023.111927.
Hangala, L.S., 1987. The early Proterozoic Zn-Pb-Cu massive sulfide deposit at Attu, SW Finland. Bull. Geol. Surv. Finl. 341, 61 p.
Harrison, C.G.A., 1994. Rates of continental erosion and mountain building. Geol. Rundsch. 83, 431–447.
Hasebe, N., Barberand, J., Jarvis, K., Carter, A., Hurford, A.J., 2004. Apatite fission-track chronometry using laser ablation ICP-MS. Chem. Geol. 207, 135–145.
Heikkinen, P., Giese, R., Kueck, J., Kukkonen, I., Malin, P., 2021. Basement-EGS Structure from VSP, Drilling, Well Logs, and Geology in Espoo. Finland. GRC Transactions 45. https://publications.mygeoenergynow.org/grc/1034472.pdf.
Heller, P.L., Angevine, C.L., Winslow, N.S., Paola, C., 1988. Two-phase stratigraphic model of foreland-basin sequences. Geology 16, 501–504.
Hendriks, B., Andriessen, P., Huigen, Y., Leighton, C., Redfield, T., Murrell, G., Gallagher, K., Nielsen, S.B., 2007. A fission track data compilation for Fennoscandia. Norw. J. Geol. 87, 143–155.
Hestnes, Å., Gasser, D., Ketcham, R., Dunkl, I., Ksienzyk, A.K., Scheiber, T., Sirevaag, H., Jacobs, J., 2024. The thermal evolution of Western Norway based on multi-sample models of an elevation transect: Implications for the formation of high elevation low-relief surfaces on an elevated rifted continental margin. Geochem. Geophys. 25, e2023GC010986. https://doi.org/10.1029/2023GC010986.
Hietala, S., Jokinen, J., Lerssi, J., Niskanen, M., Pesonen, L.J., Plado, J., 2023. Summanen structure: further geological and geophysical evidence of a meteorite impact event in Central Finland. Meteorit. Planet. Sci. 1002–1017. https://doi.org/10.1111/maps.14033.
Hölttä, P., Balagansky, V., Garde, A.A., Mertanen, S., Peltonen, P., Slabunov, A., Sorjonen-Ward, P., Whitehouse, M., 2006. Archean of Greenland and Fennoscandia. Episodes 31, 13–18.
Horsfield, B., Kieft, T.L., the GeoBiosphere Group, 2007. The GeoBiosphere. In: Harms, U., Koeberl, C. and Mark D. Zoback (eds.), Continental scientific drilling: a decade of progress, and challenges for the future, Springer, Berlin, pp. 163–212.
Hurford, A.J., 2019. A historical perspective on fission-track thermochronology. In: M.G. Malusa and P.G. Fitzgerald (Eds.), Fission-Track Thermochronology and its Application to geology, Springer, 3–23, Doi: 10.1007/978-3-319-89421-8_1.
Isozaki, Y., Põldvere, A., Bauert, H., Nakahata, H., Aoki, K., Sakata, S., Hirata, T., 2014. Provenance shift in Cambrian mid-Baltica: detrital zircon chronology of Ediacaran - Cambrian sandstones in Estonia. Est. J. Earth Sci. 63, 251–256. https://doi.org/10.3176/earth.2014.27.
Itävaara, M., Nyyssönen, M, Bomberg, M., Kapanen, A., Nousiainen, A., Ahonen, L., Hultman, J., Paulin, L., Auvinen, P., Kukkonen, I.T., 2011. Microbiological sampling and analysis of the Outokumpu Deep Drill Hole biosphere in 2007-2009. In: Kukkonen, I.T. (Ed.), Outokumpu Deep Drilling Project 2003-2010, Special Paper, 51. Geological Survey of, pp. 199–206.
Japsen, P., Chalmers, J.A., 2022. The norwegian mountains: the result of multiple episodes of uplift and subsidence. Geol. Today 38 (1), 13–19.
Japsen, P., Bidstrup, T., Lidmar-Bergström, K., 2002. Neogene uplift and erosion of southern Scandinavia induced by the rise of the South Swedish Dome. In Doré, A.G., Cartwright, J.A., Stoker, M.S., Turner, J.E., White, N., (Eds), Exhumation of the North Atlantic Margin: Timing, Mechanisms and Implications for Petroleum Exploration. Geol. Soc. London, Spec. Publ., 196, pp. 183–207.
Japsen, P., Green, P.F., Bonow, J.M., Erlström, M., 2015. Episodic burial and exhumation of the southern Baltic Shield: Epeirogenic uplifts during and after break-up of Pangaea. Gondwana Res. 35, 357–377.
Japsen, P., Green, P.F., Chalmers, J.A., Bonow, J.M., 2018. Mountains of southernmost Norway: uplifted Miocene peneplains and re-exposed Mesozoic surfaces. J. Geol. Soc. London 157, 721–741.
Jõeleht, A., Kukkonen, I.T., 1996. Heat flow density in Estonia - assessment of palaeoclimatic and hydrogeological effects. Geophysica 32, 291–317.
Jõeleht, A., Kukkonen, I.T., 2002. Physical properties of Vendian to Devonian sedimentary rocks in Estonia. GFF 124, 65–72. https://doi.org/10.1080/11035890201242065.
Juhojuntti, N., Juhlin, C., Dyrelius, D., 2001. Crustal reflectivity underneath the central Scandinavian Caledonides. Tectonophysics 334, 191–210.
Juhlin, C., Almqvist, B., Lorenz, H., Hedin, P., 2019. The collisional orogeny in the Scandinavian Caledonides (COSC) project: some results and current status. International Symposium on Deep Earth Exploration and Practices, Beijing, China – October 24–26, 2018. Acta Geol. Sin. Engl. Ed. 93, 33–35.
Kashefi, K., Lovley, D.R., 2003. Extending the upper temperature limit for life. Science 301 (5635), 934.
Ketcham, R.A., 2005. Forward and inverse modeling of low-temperature thermochronometry data. Rev. Mineral. Geochem. 58, 275–314.
Ketcham, R.A., Carter, A., Donelick, R.A., Barbarand, J., Hurford, A.J., 2007. Improved modeling of fission-track annealing in apatite. Am. Min. 92, 799–810.
Ketcham, R.A., Donelick, R.A., Balestrieri, M.L., Zattin, M., 2009. Reproducibility of apatite fission-track length data and thermal history reconstruction. Earth Plan. Sci. Lett. 284, 504–515.
Kirsimäe, K., Somelar, P., Jõeleht, A., 2020. Illitization of the lower Cambrian (Terreneuvian) Blue Clay in the northern Baltic Palaeobasin. Est. J. Earth Sci. 69, 200–213. https://doi.org/10.3176/earth.2020.14.
Kheraskova, T.N., Volozh, Y.A., Vorontsov, A.K., Pevzner, L.A., Sychkin, N.I., 2002. Sedimentation Conditions at the central east European Platform in Riphean and Early Vendian. Lithol. Miner. Resour. 37, 68–81.
Kohn, B.P., Lorencak, M., Gleadow, A.J.W., Kohlmann, F., Raza, A., Osadetz, K.G., Sorjonen-Ward, P., 2009. A reappraisal of low-temperature thermochronology of the eastern Fennoscandia Shield and radiation-enhanced apatite fission-track annealing. In: Lisker, F., Ventura, B., Glasmacher, U.A., (eds.), Thermochronological Methods: From Palaeotemperature Constraints to Landscape Evolution Models. Geol. Soc. London, Spec. Publ. 324, 193–216. DOI: 10.1144/SP324.15 0305-8719/09.
Kohn, B., Gleadow, A., 2019. Application of low-temperature thermochronology to craton evolution. In: Malusa, M.G., Fitzgerald, P.G., (Eds.), Fission-Track Thermochronology and its Application to geology, Springer, 373–393, Doi: 10.1007/978-3-319-89421-8_21.
Kohn, B.P., Ketcham, R.A., Vermeesch, P., Boone, S.C., Hasebe, N., Chew, D., Bernet, M., Chung, L., Danišík, M., Gleadow, A.J.W., Sobel, E.R., 2024. Interpreting and reporting fission-track chronological data. Geol. Soc. Am. b. 136, 3891–3920. https://doi.org/10.1130/B37245.1.
Kohonen, J., Rämö, O.T., 2005. Sedimentary rocks, diabases, and late cratonic evolution. In: Lehtinen, M., Nurmi, P., Rämö, T. (Eds.), The Precambrian Bedrock of Finland - Key to the Evolution of the Fennoscandian Shield. Elsevier, pp. 563–604.
Kohonen, J., Pihlaja, P., Kujala, H., Marmo, J., 1993. Sedimentation of the Jotnian Satakunta sandstone, western Finland. Bull. Geol. Surv. Finl. 369, 34 p.
Koistinen, T. (ed.), 1994, Precambrian basement of the Gulf of Finland and surrounding area, 1:1 mill. Geol. Surv. Finl., Espoo. https://tupa.gtk.fi/kartta/erikoiskartta/ek_031.pdf.
Koistinen, T., Stephens, M. B., Bogatchev, V., Nordgulen, Ø. Wennerström, M., Korhonen, J., 2001, Geological map of the Fennoscandian Shield, scale 1:2 000 000: Geological Surveys of Finland, Norway and Sweden and the North-West Department of Natural Resources of Russia.
Komiya, T., Yamamoto, S., Aoki, S., Sawaki, Y., Ishikawa, A., Tashiro, T., Koshida, K., Shimojo, M., Aoki, K., Collerson, K.D., 2015. Geology of the Eoarchean, >3.95 Ga, Nulliak supracrustal rocks in the Saglek Block, northern Labrador, Canada: the oldest geological evidence for plate tectonics. Tectonophysics 662, 40–66. https://doi.org/10.1016/j.tecto.2015.05.003.
Kranendonk, M.J., 2011. Onset of Plate Tectonics. Science 333, 413–414.
Kristoffersen, M., Andersen, T., Andresen, A., 2014. U–Pb age and Lu–Hf signatures of detrital zircon from Palaeozoic sandstones in the Oslo Rift. Norway. Geol. Mag. 151, 816–829. https://doi.org/10.1017/S0016756813000885.

Kukkonen, I.T., 1993. Heat flow map of northern and central parts of the Fennoscandian Shield based on geochemical surveys of heat producing elements. Tectonophysics 225, 3–13.
Kukkonen, I.T., Jõeleht, A., 1996. Geothermal modelling of the lithosphere in the central Baltic Shield and its southern slope. Tectonophysics 255, 25–45.
Kukkonen, I.T., Jõeleht, 2003. Weichselian temperatures from geothermal heat flow data. J. Geophys. Res. 108 (B3). ETG-9, pp. 11.
Kukkonen, I.T., Lauri, L.S., 2009. Modelling the thermal evolution of a collisional Precambrian orogen: high heat production migmatitic granites of southern Finland. Precambr. Res. 168, 233–246.
Kukkonen, I.T., Kuusisto, M., Lehtonen, M., Peltonen, P., 2008. Delamination of eclogitized lower crust: Control on the crust–mantle boundary in the central Fennoscandian shield. Tectonophysics 457, 111–127.
Kukkonen, I.T., Heikkinen, P.J., Malin, P.E., Renner, J., Dresen, G., Karjalainen, A., Rytkönen, J., Solantie, J., 2023. Hydraulic conductivity of the crystalline crust: Insights from hydraulic stimulation and induced seismicity of an enhanced geothermal system pilot reservoir at 6 km depth, Espoo, southern Finland. Geothermics 112, 102743. https://doi.org/10.1016/j.geothermics.2023.102743.
Kuusirati, J., Toropainen, V., 2015. Luotausreiän OTN-1 kairausnäytteiden kivilajitulkinta sekä valokuvaaminen. Drillcon SMOY, report 3054/A/2015/JK, VT to St1, 9 p., 3 app. (in Finnish,' Lithological interpretation and photography of the OTN-1 drill cores').
Kyle, J.E., Eydal, H.S.C., Ferris, F.G., Pedersen, K., 2008. Short communication. Viruses in granitic groundwater from 69 to 450 m depth of the äspö hard rock laboratory. Sweden. ISME J 2, 571–574.
Lachenbruch, A.H., Morgan, P., 1990. Continental extension, magmatism and elevation; formal relations and rules of thumb. Tectonophysics 174, 39–62.
Lahtinen, R., Köykkä, J., Salminen, J., Sayab, M., Johnston, S.T., 2023. Paleoproterozoic tectonics of Fennoscandia and the birth of Baltica. Earth Sci. Rev. 246, 104586. https://doi.org/10.1016/j.earscirev.2023.104586.
Larson, S.A., Tullborg, E.-L., 1998. Why Baltic Shield zircons yield late Paleozoic, lower-intercept ages on U-Pb concordia. Geology 26, 919–922.
Larsen, B.T., Olaussen, S., Sundvoll, B., Heeremans, M., 2008. The Permo-Carboniferous Oslo Rift through six stages and 65 million years. Episodes Journal of International Geoscience 31 (1), 52–58.
Larson, S.A., Cederbom, C.E., Tullborg, E.-L., Stiberg, J.-P., 1999. Sveconorwegian and Caledonian foreland basins in the Baltic Shield revealed by fission track thermochronology. Terra Nova 11, 210–215.
Lehtinen, M., Nurmi, P.A., Rämö, O.T., 2005. Precambrian Geology of Finland – Key to the evolution of the Fennoscandian Shield. Elsevier B.V, Amsterdam, p. 720.
Lehtovaara, J., 1976. Apatite fission track dating of finnish Precambrian intrusives. Ann. Acad. Sci. Fenn. 117, 1–94.
Leventhal, J.S., 1991. Comparison of organic geochemistry and metal enrichment in two black shales: Cambrian Alum Shale of Sweden and Devonian Chattanooga Shale of United States. Mineral. Deposita 26, 104–112.
Li, Z.X., Bogdanova, S.V., Collins, A.S., Davidson, A., De Waele, B., Ernst, R.E., Fitzsimons, I.C.W., Fuck, R.A., Gladkochub, D.P., Jacobs, J., Karlstrom, K.E., Lul, S., Natapovm, L.M., Pease, V., Pisarevsky, S.A., Thrane, K., Vernikovsky, V., 2008. Assembly, configuration, and break-up history of Rodinia: a synthesis. Precambr. Res. 160, 179–210.
Lidmar-Bergström, K., 1995. Relief and saprolites through time on the Baltic Shield. Geomorphology 12, 45–61.
Lidmar-Bergström, K., 1996. Long term morphotectonic evolution in Sweden. Geomorphology 16, 33–59.
Lidmar-Bergström, K., Bonow, J.M., 2009. Hypotheses and observations on the origin of the landscape of southern Norway—A comment regarding the isostasy-climate-erosion hypothesis by.
Lidmar-Bergström, K., Näslund, J.O., 2002. Landforms and uplift in Scandinavia. In: Doré, A.G., Cartwright, J.A., Stoker, M.S., Turner, J.P., White, N. (Eds.), Exhumation of the North Atlantic Margin: Timing, Mechanisms and Implications for Petroleum Exploration, vol. 196. Geol. Soc. London, Spec. Publ., pp. 103–116.
Lidmar-Bergström, K., Ollier, C.D., Sulebak, J.R., 2000. Landforms and uplift history of southern Norway. Global Planet. Change 24, 211–231.
Lidmar-Bergström, K., Bonow, P., Japsen, P., 2013. Stratigraphic Landscape Analysis and geomorphological paradigms: Scandinavia as an example of Phanerozoic uplift and subsidence. Global Planet. Change 100, 153–171.
Lin, L.-H., Slater, G.F., Lollar, B.S., Lacrampe-Couloume, G., Onstott, T., 2005. The yield and isotopic composition of radiolytic H_2, a potential energy source for the deep subsurface biosphere. Geochim. Cosmochim. Acta 69, 893–903.
Lorencak, M., 2003. Low Temperature Thermochronology of the Canadian and Fennoscandian Shields: Integration of Apatite Fission Track and (U–Th)/He Methods. University of Melbourne. PhD thesis.
Magnabosco, C., Lin, L.-H., Dong, H., Bomberg, M., Ghiorse, W., Stan-Lotter, H., Pedersen, K., Kieft, T.L., Van Heerden, E., Onstott, T.C., 2018. The biomass and biodiversity of the continental subsurface. Nat. Geosci. 2018 (11), 707–717.
Masaitis, V.L., 2005. Morphological, structural and lithological records of terrestrial impacts: an overview. Aust. J. Earth Sci. 52, 509–528. https://doi.org/10.1080/08120090500170427.
Matmon, A., Bierman, P.R., Larsen, J., Southworth, S., Pavich, M., Caffee, M., 2003. Temporally and spatially uniform rates of erosion in the southern Appalachian Great Smoky Mountains. Geology 31, 155–158.
Maupin, V., 2011. Upper-mantle structure in southern Norway from beamforming of Rayleigh wave data presenting multipathing. Geophys. J. Int. 185, 985–1002.
McMahon, S., Parnell, J., 2014. Weighing the deep continental biosphere. FEMS Microbiol. Ecol. 87, 113–120.
Meert, J.G., Walderhaug, H.J., Torsvik, T.H., Hendriks, B.W.H., 2007. Age and paleomagnetic signature of the Alnø carbonatite complex (NE Sweden): additional controversy for the Neoproterozoic paleoposition of Baltica. Precambr. Res. 154, 159–174.
Medhus, A.B., Balling, N., Jacobsen, B.H., Weidle, C., England, R.W., Kind, R., Thybo, H., Voss, P., 2012. Upper-mantle structure beneath the Southern Scandes Mountains and the Northern Tornquist Zone revealed by P-wave traveltime tomography. Geophys. J. Int. 189, 1315–1334.
Melosh, H.J., 1989. Impact Cratering – a Geologic Process. Oxford University Press, New York, p. 245.
Merdith, A.S., Williams, S.E., Collins, A.S., Tetley, M.G., Mulder, J.A., Blades, M.L., Young, A., Armistead, S.E., Cannon, J., Zahirovic, S., Müller, R.D., 2021. Extending full-plate tectonic models into deep time: linking the Neoproterozoic and the Phanerozoic. Earth Sci. Rev. 214, 103477. https://doi.org/10.1016/j.earscirev.2020.103477.
Mertanen, S., Airo, M.-L., Elminen, T., Niemelä, R., Pajunen, M., Wasenius, P., Wennerström, M., 2008. Paleomagnetic evidence for Mesoproterozoic – Paleozoic reactivation of the Paleoproterozoic crust in southern Finland. Geol. Surv. Finl. Spec. Paper 47, 215–252.
Morley, C.K., 1986. The Caledonian thrust front and palinspastic restorations in the southern Norwegian Caledonides. J. Struct. Geol. 8, 753–765.
Morley, C.K., 1992. Hydrocarbon generation - a possible cause of elevated pore pressures in the Osen-Røa thrust sheet. Norway. J. Struct. Geology 14, 743–747.
Murray, K.E., Stevens Goddard, A.L., Abbey, A.L., Wildman, M., 2022. Thermal history modeling techniques and interpretation strategies: applications using HeFTy. Geosphere 18, 1622–1642. https://doi.org/10.1130/GES02500.1.
Murrell, G.R., 2003. The long-term thermal Evolution of Central Fennoscandia. Vrjie Universiteit, Amsterdam. PhD thesis.
Murrell, G.L., Andriessen, P.A.M., 2004. Unravelling a long-term multi-event thermal record in the cratonic interior of southern Finland through apatite fission track thermochronology. Phys. Chem. Earth 29, 695–706.
Mosar, J., Torsvik, T., the BAT team, 2002. Opening the Norwegian and Greenland Seas: Plate tectonics of Mid Norway since the Late Permian. In: Eide, (coord.), et al. (Eds.), BATLAS - Mid Norway Plate Reconstruction Atlas with Global and Atlantic Perspectives. Geol. Surv, Norway, pp. 48–59.
Müller, R., Petter Ngstuen, J., Eide, F., Lie, H., 2005. Late Permian to Triassic basin infill history and palaeogeography of the Mid-Norwegian shelf-East Greenland region. Norw. Petroleum Soc. Spec. Publ. 12, 165–189. https://doi.org/10.1016/S0928-8937(05)80048-7.
Nielsen, A.T., Schovsbo, N.H., 2011. The lower Cambrian of Scandinavia: depositional environment, sequence stratigraphy and palaeogeography. Earth Sci. Rev. 107, 207–310. https://doi.org/10.1016/j.earscirev.2010.12.004.
Nielsen, S.B., Gallagher, K., Leighton, C., Balling, N., Svenningsen, L., Jacobsen, B.H., Thomsen, E., Nielsen, O.B., Heilmann-Clausen, C., Egholm, D.L., Summerfield, M.A., Clausen, O.R., Piotrowski, J.A., Thorsen, M.R., Huuse, M., Abrahamsen, N., King, C., Lykke-Andersen, H., 2009a. The evolution of western Scandinavian topography: a review of Neogene uplift versus the ICE (isostacy-climate-erosion) hypothesis. J. Geodyn. 47, 72–95.
Nielsen, S.B., Gallagher, K., Egholm, D.L., Clausen, O.R., Summerfield, M., 2009b. Reply to comment regarding the ICE-hypothesis. J. Geodyn. 48, 101–106.
Nikishin, A.M., Ziegler, P.A., Stephenson, R.A., Cloething, S.A.P.L., Furne, A.V., Foki, P. A., Ershov, A.V., Bolotov, S.N., Korotaev, M.V., Alekseev, A.S., Gorbachev, V.I., Shipilov, E.V., Lankreijer, A., Bembinova, E.Y., Shalimov, I.V., 1996. Late Permian to Triassic history of the east European Craton dynamics of sedimentary basin evolution. Tectonophysics 268, 23–63.
Nironen, M., 1997. The Svecofennian Orogen: a tectonic model. Precamb. Res. 86, 21–44.
Nuppunen-Puputti, M., Kietävainen, R., Purkamo, L., Rajala, P., Itävaara, M., Kukkonen, I., Bomberg, M., 2021. Rock surface fungi in deep continental biosphere-exploration of microbial community formation with subsurface in situ biofilm trap. Microorganisms 9, 64. https://doi.org/10.3390/microorganisms9010064.
O'Brien, H.E., Peltonen, P., Vartiainen, H., 2005. Kimberlites, carbonatites, and alkaline rocks. In: Lehtinen, M., Nurmi, P.A., Rämö, O.T. (Eds.), 2005. Precambrian Geology of Finland – Key to the evolution of the Fennoscandian Shield. Elsevier B.V. Amsterdam, pp. 605-644.
Oliver, J., 1986. Fluids expelled tectonically from orogenic belts: their role in hydrocarbon migration and other geologic phenomena. Geology 14, 99–102.
Onstott, T.C., Phelps, T.J., Kieft, T., Colwell, F.S., Balkwill, D.L., Fredrickson, J.K., Brockman, F.J., 1999. A global perspective on the microbial abundance and activity in the deep subsurface. In: Seckbach, J. (Ed.), Enigmatic Microorganisms and Life in Extreme Environments. Kluwer, Dordrecht, pp. 489–501.
Obst, K., Solyom, Z., Johansson, L. 2004. Permo-Carboniferous extension-related magmatism at the SW margin of the Fennoscandian Shield. In: Wilson, M., Neumann, E.-R., Davies, G.R., Timmermann, M.J., Heeremans, M., Larsen, B.T. (eds), Permo-Carboniferous Magmatism and Rifting in Europe. Geol. Soc.i London, Spec. Publ. 223, 259-288.
Ouimet, W.B., Whipple, K.X., Granger, D.E., 2009. Beyond threshold hillslopes: Channel adjustment to base-level fall in tectonically active mountain ranges. Geology 37, 579–582.
Paradis, S., Hannigan, P., Dewing, K., 2007, Mississippi Valley-type lead-zinc deposits, in Goodfellow, W.D., ed., Mineral Deposits of Canada: A Synthesis of Major Deposit-Types, District Metallogeny, the Evolution of Geological Provinces, and Exploration Methods: Geological Association of Canada, Mineral Deposits Division, Special Publication No. 5, pp. 185–203.
Pedersen, K., 1997. Microbial life in deep granitic rock. FEMS Microbiol. Rev. 20, 399–414.

Pedersen, K., 2000. Exploration of deep intraterrestrial microbial life: current perspectives. FEMS Microbiol. Lett. 185 (9–16), 2000.
Pedersen, V.K., Braun, J., Huismans, R.S., 2018. Eocene to mid-Pliocene landscape evolution in Scandinavia inferred from offshore sediment volumes and pre-glacial topography using inverse modelling. Geomorphology 303, 467–485. https://doi.org/10.1016/j.geomorph.2017.11.025.
Pesonen, L.J., Elming, S.-Å., Mertanen, S., Pisarevsky, S., D'Agrella-Fillho, M.S., Meert, J. G., Schmidt, P.W., Abrahamsen, N., Bylund, G., 2003. Palaeomagnetic configuration of continents during the Proterozoic. Tectonophysics 375, 289–324.
Perens, R., Vallner, L., 1997. Water-bearing formation. In: Raukas, A., Teedumäe, A., (Eds.), Geology and mineral resources of Estonia. Est. Acad. Publishers, Tallinn, pp. 137–145.
Petrov, O.V., Morozov, A.F., Shatov, V.V., Molchanov, A.V., Terekhov, A.V., Lukyanova, L.I., Artem'ev, D.S., Belova, V.N. and Khalenev, V.O., 2016. Chapter 9: Russia. Mineral Resources in the Arctic: Skien, NGU-Geol. Surv. Norway, pp.373–482.
Peulvast, J.-P., 1985. Post-orogenic morphotectonic evolution of the Scandinavian Caledonides during the Mesozoic and Cenozoic. In: Gee, D.G., Sturt, B.A. (Eds.), The Caledonide Orogen—Scandinavia and Related Areas. Wiley, Chichester, pp. 979–996.
Peyton, S.L., Carrapa, B., 2013, An introduction to low-temperature thermochronologic techniques, methodology, and applications. In: Knight, C., Cuzella, J., (eds.), Application of structural methods to Rocky Mountain hydrocarbon exploration and development, AAPG Stud. Geol. 65, pp. 15–36.
Phillips, J.D., 2002. Erosion, isostatic response, and the missing peneplains. Geomorphology 45, 225–241.
Pichugin, M.S., Puura, V.A., Vingisaar, P.A., Erisalu, E.K., 1977. Regional metasomatic dolomitization associated with tectonic disturbances in lower Paleozoic deposits of the Northern Baltic region. Int. Geol. Rev. 19, 903–912. https://doi.org/10.1080/00206817709471088.
Plado, J., Preeden, U., Pesonen, L.J., Mertanen, S., Puura, V., 2010. Magnetic history of Early and Middle Ordovician sedimentary sequence, northern Estonia. Geophys. J. Int. 180, 147–157.
Platt, J.P., England, P.C., 1993. Convective removal of lithosphere beneath mountain belts: thermal and mechanical consequences. Am. J. Sci. 293, 307–336.
Plink-Björklund, P., Björklund, L., 1999. Sedimentary response in the Baltic Devonian Basin to post-collisional events in the Scandinavian Caledonides. GFF 121, 79–80.
Plomerová, J., Babuška, V., 2010. Long memory of mantle lithosphere fabric — European LAB constrained from seismic anisotropy. Lithos 120, 131–143.
Põldvere, A., Isozaki, Y., Bauert, H., Aoki, K., Sakata, S., Hirata, T., 2014. Provenance of the lower - Middle Paleozoic of Estonia in central Baltica: a possible link to Avalonia. GFF 136, 214–217.
Poprawa, P., Šliaupa, S., Stephenson, R.A., Lazauskiene, J., 1999. Late Ediacaran–Early Palaeozoic tectonic evolution of the Baltic basin: regional implications from subsidence analysis. Tectonophysics 314, 219–239.
Preeden, U., Mertanen, S., Elminen, T., Plado, J., 2009. Secondary magnetizations in shear and fault zones in southern Finland. Tectonophysics 479, 203–213.
Puura, V., Plado, J., 2005. Settings of meteorite impact structures in the Svecofennian crustal domain. In: Koeberl, C., Henkel, H. (Eds.), Impact Tectonics. Springer, pp. 211–245.
Ranalli, G., 1995. Rheology of the Earth. Chapman and Hall, London, p. 413.
Rämö, O.T., Haapala, I., 2005. Rapakivi granites. In: Lehtinen, M., Nurmi, P.A., Rämö, O. T. (Eds.), Precambrian Geology of Finland–Key to the Evolution of the Fennoscandian Shield. Developments in Precambrian Geology, vol. 14. Elsevier B.V., Amsterdam, pp. 533–562.
Raukas, A., Teedumäe, A. (Eds.), 1997. Geology and Mineral Resources of Estonia. Est. Acad. Publ, Tallinn, p. 436.
Reijonen, H.M., Al-Ani, T., Kuva, J., Elminen, T., Issukka, K., Lamminmäki, R., 2024. Fracture smectites in bedrock at Kivetty and Romuvaara sites, Finland as natural analogues for radioactive waste repository buffer. Geoenergy 2, geoenergy2023-053. https://doi.org/10.1144/geoenergy2023-053.
Reiners, P.W., Brandon, M.T., 2006. Using thermochronology to understand orogenic erosion. Annu. Rev. Earth Planet. Sci. 34, 419–466.
Riis, F., 1996. Quantification of Cenozoic vertical movements of Scandinavia by correlation of morphological surfaces with offshore data. Global Planet. Change 12, 331–357.
Roberts, D., 2003. The Scandinavian Caledonides: event chronology palaeogeographic setting and likely modern analogues. Tectonophysics 365, 283–299.
Rohrman, M., 1995. Thermal evolution of the Fennoscandian region from fission track thermochronology. Vrije Universiteit Amsterdam. PhD thesis.
Rohrman, M., van der Beek, P.A., van der HIlst, R.D., Reemst, P., 2002. In: Doré, A.G., Cartwright, J.A., Stoker, M.S., Turner, J.E., White, N. (Eds.), Geol. Soc. London, Spec. Publ. 196, 27–43.
Sahl, J.W., Schmidt, R., Swanner, E.D., Mandernack, K.W., Templeton, A.S., Kieft, T.L., Smith, R.L., Sanford, C.R.L., Mitton, J.B., Spear, J.R., 2008. Subsurface microbial diversity in deep-granitic fracture water in Colorado. Appl. Environ. Microb. 74, 143–152.
Saksa, P., Front, K., Ahokas, H., Lindh, J., 1998. Investigations of the crushed fracture zone encountered in the borehole KR5 at Kivetty. Work Report 98-32. Posiva Oy, Helsinki. 49 p. (in Finnish).
Samuelsson, J., Middleton, M.F., 1998. The Caledonian foreland basin in Scandinavia: constrained by thermal maturation of the Alum Shale. GFF 120, 307–314.
Sandström, B., Tullborg, E.-L., De Torres, T., Ortiz, J.E., 2006. The occurrence and potential origin of asphaltite in bedrock fractures. Forsmark, Central Sweden, GFF 128, 233–242. https://doi.org/10.1080/11035890601283233.
Schön, J. H., 2004. Physical Properties of Rocks: Fundamentals and Principles of Petrophysics, Elsevier, pp. 583.
Schulz, H.-M., Yang, S., Schovsbo, N.H., Rybacki, E., Ghanizadeh, A., Bernard, S., Mahlstedt, N., Krüger, M., Amann-Hildebrandt, A., Krooss, B.M., Meier, T., Reinicke, A., 2021. The Furongian to lower Ordovician Alum Shale Formation in conventional and unconventional petroleum systems in the Baltic Basin – a review. Earth Sci. Rev. 218, 103674. https://doi.org/10.1016/j.earscirev.2021.103674.
Seiler, C., Boone, S.C., Kohn, B.P., Gleadow, A.J., 2023. A grain-by-grain comparison of apatite fission-track analysis by LA-ICP-MS and the external detector method. Chem. Geol. 635, 121623.s. https://doi.org/10.1016/j.chemgeo.2023.121623.
Seranne, M., Seguret, M., 1987. The Devonian basins of western Norway: tectonics and kinematics of an extending crust. In: Coward, M.P., Dewey, J.F. & Hancock, P.L. (eds), Continental Extensional Tectonics, Geol. Soc. Spec. Publ. 28, 537–548.
Simonen, A., Kouvo, O., 1955. Sandstones in Finland. Compt. Rend. Soc. Geol. Finlande 28, 58–87.
Somelar, P., Kirsimäe, K., Środoń, J., 2009. Mixed layer illite-smectite in the Kinnekulle K-bentonite, northern Baltic Basin. Clay Miner. 44, 455–468.
Somelar, P., Kirsimäe, K., Hints, R., Kirs, J., 2010. Illitization of Early Paleozoic K-bentonites in the Baltic Basin: decoupling of burial and fluid driven processes. Clays Clay Miner. 58, 388–398.
Söderman, G., 1985. Planation and weathering in eastern Fennoscandia. Fennia 163, 345–352.
Söderman, G., Kejonen, A., Kujansuu, R., 1983. The riddle of the tors at Lauhavuori, western Finland. Fennia 161, 91–144.
Środoń, J., Clauer, N., Huff, W., Dudek, T., Banas, M., 2009. K-Ar dating of the lower Palaeozoic K-bentonites from the Baltic Basin and the Baltic Shield: implications for the role of temperature and time in the illitization of smectite. Clay Miner. 44, 361–387.
Šliaupa, S., Hoth, P., 2011. Geological Evolution and Resources of the Baltic Sea Area from the Precambrian to the Quaternary. In: J. Harff et al. (eds.), The Baltic Sea Basin, Central and Eastern European Development Studies (CEEDES), p. 13–51, doi 10.1007/978-3-642-17220-5_2.
Steckler, M.S., Omar, G.I., Kamer, G.D., Kohn, B.P., 1993. Pattern of hydrothermal circulation within the Newark basin from fission-track analysis. Geology 21, 735–738.
Steel, R. J., 1993. Triassic-Jurassic megasequence stratigraphy in the northern North Sea: Rift to post-rift evolution. In: Geological Society, London, Petroleum Geology Conference Series 4, no. 1, pp. 299–315. Doi: 10.1144/0040299.
Stephens, M.B., Weihed, P., 2013.Tectonic evolution and mineral resources in the Fennoscandian Shield, Sweden. In: Allen, R., Jansson N., Ripa, M., (eds.), Bergslagen: Geology of the volcanic- and limestone-hosted base metal and iron oxide deposits. Geol. Surv. Sweden, SGA excursion guidebook SWE4, 10–20.
Sundblad, K., Kivisilla, J., Puura, V., Jonsson, E., Fedorenko, J., 1999. Palaeozoic Pb (±Zn) mineralization in the Baltic Sea region. GFF 121, 76–77.
Suuroja, K., Suuroja, S., 2002. Neugrund Structure - the Newly Discovered Submarine Early Cambrian Impact Crater. In: Gilmour, I., Koeberl, C. (Eds.), Impacts and the early Earth, Lecture notes in Earth Sciences 91, 389–416.
Svensen, H., Jamtveit, B., 1998. Contact metamorphism of shales and limestones from the Grua area, the Oslo Rift, Norway: a phase-petrological study. Norw. J. Geol. 78, 81–98.
Takai, K., Moser, D.P., De Flaun, M., Onstott, T.C., Fredrickson, J.K., 2001. Archaeal diversity in waters from deep South African Gold Mines. Appl. Environ. Microb. 67, 5750–5760.
Timmerman, M.J., Heeremans, M., Kirstein, L.A., Larsen, B.T., Spencer-Dunworth, E.-A., Sundvoll, B., 2009. Linking changes in tectonic style with magmatism in northern Europe during the late Carboniferous to latest Permian. Tectonophysics 473, 375–390.
Torsvik, T.H., Cocks, L.R.M., 2005. Norway in space and time: a Centennial cavalcade. Norw. J. Geol. 85, 73–86.
Torsvik, T.H., Smethurst, M.A., Meert, J.G., Van der Voo, R., McKerrow, W.S., Brasier, M. D., Sturt, B.A., Walderhaug, H.J., 1996. Continental break-up and collision in the Neoproterozoic and Palaeozoic – a tale of Baltica and Laurentia. Earth Sci. Rev. 40, 229–258.
Torsvik, T.H., Van der Voo, R., Meert, J.G., Mosar, J., Walderhaug, H.J., 2001. Reconstructions of the continents around the North Atlantic at about the 60th parallel. Earth Plan. Sci. Lett. 187, 55–69.
Tšeban, T.H., 1975. Eesti NSV põhjavesi ja selle kasutamine. Valgus, Tallinn, 166 p. (in Estonian).
Tucker, G.E., 2015. Landscape Evolution. Treatise on Geophysics, Second Ed., p. 593–630. Doi: 10.1016/B978-0-444-53802-4.00124-X.
Tullborg, E.-L., Larson, S.Å, Björklund L., Stigh, J., 1995. Thermal evidence of Caledonide foreland, molasse sedimentation in Fennoscandia. Swedish Nuclear Fuel and Waste Management CO, SKB technical report 95-18, 38 pp. https://www.skb.com/publication/12024/TR95-18_OCR.pdf).
Turcotte, D.L., Schubert, G., 2014. Geodynamics, third ed. Cambridge Univ. Press, pp. 623.
Tuuling, I., 2019. The Leba Ridge–Riga–Pskov Fault Zone – a major East European Craton interior dislocation zone and its role in the early Palaeozoic development of the platform cover. Est. J. Earth Sci. 68, 161–189. https://doi.org/10.3176/earth.2019.12.
Tynni, R., Hokkanen, K., 1982. Annelidien ryömimisjälkiä Lauhanvuoren hiekkakivessä. Summary: traces of crawling by annelids in Lauhanvuori sandstone. Geologi 34, 129–134.
Vaher, R.M., Puura, V.A., Erisalu, E.K., 1961. Tectonic structure of northeastern Estonia. In: Geology of the Paleozoic, Trudy Inst. Geol. Ann. Est. SSR, v. 10, Valgus, Tallinn.
Veikkolainen, T., Kukkonen, I.T., 2019. Highly varying radiogenic heat production in Finland, Fennoscandian Shield. Tectonophysics 750, 93–116. https://doi.org/10.1016/j.tecto.2018.11.006.

Vermeesch, P., 2017. Statistics for LA-ICP-MS based fission track dating. Chem. Geol. 456, 19–27. https://doi.org/10.1016/j.chemgeo.2017.03.002.
Vermeesch, P., Tian, Y., 2014. Thermal history modelling: HeFTy vs. Qtqt. Earth Sci. Rev. 139 (279–290), 2014.
Walsh, E.O., Hacker, B.R., Gans, P.B., Wong, M.S., Andersen, T.B., 2013. Crustal exhumation of the western gneiss region UHP terrane, Norway: $^{40}Ar/^{39}Ar$ thermochronology and fault-slip analysis. Tectonophysics 608, 1159–1179. https://doi.org/10.1016/j.tecto.2013.06.030.
Wannäs, K.O., 1989. Seismic stratigraphy and tectonic development of the Upper Proterozoic to lower Paleozoic of the Bothnian Bay, Baltic Sea. Stockh. Contrib. Geol. 40, 83–168.
Weidle, C., Maupin, V., Ritter, J., Kværna, T., Schweitzer, J., Balling, N., Thybo, H., Faleide, J.I., Wenzel, F., 2010. MAGNUS - a seismological broadband experiment to resolve crustal and upper mantle structure beneath the Southern Scandes Mountains in Norway. Seismol. Res. Lett. 81, 76–84.
Whitman, W.B., Coleman, D.C., Wiebe, W.J., 1998. Prokaryotes: the unseen majority. Proc. Natl. Acad. Sci. U.S.A. 95, 6578–6583.
Windley, B.F., Kusky, T., Polat, A., 2021. Onset of plate tectonics by the Eoarchean. Precambr. Res. 352, 105980. https://doi.org/10.1016/j.precamres.2020.105980.
Winterhalter, B., 1972. On the geology of the Bothnian Sea, an epeiric sea that has undergone Pleistocene glaciation. Bull. Geol. Surv. Finland 258, 66 p.
Wünnemann, K., Ivanov, B.A., 2003. Numerical modelling of the impact crater depth–diameter dependence in an acoustically fluidized target. Planet. Space Sci. 51, 831–845.